Three Problems in Astrophysical Dynamics

Thesis by

Stephen A. Slutz

In Partial Fulfillment of the Requirements

for the Degree of

Doctor of Philosophy

California Institute of Technology

Pasadena, California

1979

(Submitted November 15, 1978)

Acknowledgements

Graduate study at Caltech has not always been pleasant, but it has always been a period of growth for me both professionally and personally. I thank all of the people who contributed to the unique experience that Caltech has been.

I sincerely thank Jim Gunn, my advisor, for both the freedom to find things out by myself, and the encouragement and advice he gave me when I needed it.

I thank my friends for their support. In particular I thank Ian Gatley, Vincent Icke, Eric Persson and Steven Beckwith for their ideas and enthusiasms which helped my research efforts.

I thank Peter Goldreich for many interesting discussions and Donna Lathrop for the careful typing of this document.

My graduate study has been supported by the Fannie and John Hertz Foundation, Caltech through both teaching and research assistantships, and the NSF under contract AST75-01398 A01.

Abstract

Three dynamical problems in astrophysics are attacked. These are:

1. Radiation Pressure on Dust Grains near the Galactic Center,

It is shown that radiation pressure may drive interstellar dust grains out of the galactic center. This explains the observed density distribution of dust in this region,

2. The Acceleration of Shock Waves in the Atmospheres of Cool Mira Variable Giants,

It is shown that shocks may accelerate as they propagate outward, but not indefinitely. They reach a terminal velocity which is approximately 25 km s^{-1} for stars with surface temperatures cooler than 2400 K,

and

3. Violent Relaxation and the Infall of Gas into Cluster of Galaxies.

The infall problem is reviewed with the inclusion of the time dependence of the gravitational field. The controversy over the temperature distribution of the gas after infall is resolved. Thus the constraint on the contribution of the gas outside of clusters of galaxies toward the total density of the universe is restored to $\Omega_g < .1$.

Table of Contents

Introduction

The astrophysical problems in this thesis may seem somewhat unrelated, but that depends on your viewpoint. Cosmological theories attempt to predict the ultimate fate of the universe. The theoretical predictions depend on parameters that must be measured. Many of these observational tests depend on the details of galaxy formation, which is intimately connected to the stellar mass cycle. The first two problems concern different phases of the stellar mass cycle, while the last problem is directly related to the measurement of the density parameter Ω which is one of the cosmological variables.

Chapter 1

Radiation Pressure on Dust Grains near the Galactic Center

Abstract

The collective radiation pressure due to the cluster of stars at the galactic center may drive grains outward. The conditions for this to occur are consistent with our current observational information about this region. The drag on grains due to a stochastic galactic magnetic field is calculated and used to predict the distribution of grains. A uniform distribution results, in agreement with the infrared observations. The grain flows are unstable and the implications for the formation of Dark Clouds are briefly considered.

I. Introduction

Our view of the galactic center is obscured by thick clouds of dust and gas, presumably formed from the ejecta of evolved stars. We need to know where this dust and gas are going if we hope to understand the continuing star formation and metal production of this very active region. In particular, the motion of the dust grains relative to the gas is considered. There are several reasons why the motion of the dust is particularly interesting. The dust grains contain most of the heavy elements, they are an important cooling agent during the early phases of star formation, and they are the dominant source of opacity at visible wavelengths. Indeed, observational evidence indicates that the distributions of dust and gas are dissimilar within 10 pc of the galactic center (Gatley et al., 1977).

The physical conditions at the galactic center are poorly known due to the large (~ 27 m) of extinction produced by intervening dust (Becklin and Neugebauer, 1968). However, through infrared, radio and molecular line observations, a crude picture of physical conditions emerges.

Infrared observations at 2.2 μ suggest that the nucleus of the galaxy consists of a cluster of predominantly late type stars whose density distribution is approximately proportional to the inverse square of the distance from the center (Becklin and Neugebauer, 1968). We adopt the mass density distribution

$$\rho_*(r) = \rho_*^o \left(\frac{r_o}{r}\right)^2 M_\odot/pc^3$$

$$; \rho_*^o = 7.6 \times 10^5 M_\odot/pc^3 \qquad (1.1)$$

where r_o = 1pc. This distribution is similar to that derived by Sanders and Lowinger (1972) except that we have assumed spherical symmetry instead of the slightly flattened distribution they derive. This should not drastically influence the results since we will deal with motions near the galactic plane.

Some of these stars lose mass. Balick and Sanders (1974) estimate that the mass loss rate within the central parsec is 1.5×10^{-6} $M_\odot$/yr. The spatial dependence of the mass loss rate should follow the mass density distribution thus:

$$\Gamma(r) = \Gamma^{o}(\frac{r_o}{r})^2 \quad \text{with} \quad \Gamma^{o} \simeq 10^{-36} \text{ gm cm}^{-3} \text{ s}^{-1} \ . \tag{1.2}$$

By assuming a normal gas to dust ratio, of 100 by mass, we may also estimate the source function for grains, $\Gamma_g(r) = .01\ \Gamma(r)$. This mixture of gas and dust must eventually fall toward the galactic plane as can be seen from the following argument.

The velocity distribution which supports the stars against gravity has both a random pressure-like component and an average rotation about the center. It is the random component which keeps the stars from collapsing into a disk and it is the rotational component which causes the degree of flattening that is observed. Ejecta from stars will collide inelastically with the ejecta from other stars and lose the random component. We can estimate the time scale for this to occur as follows. Consider an expanding gas cloud of radius $r_c = V_e t$ centered on a star ejecting material at the velocity $V_e \approx 20$ km/sec. The material freely expands until the gas collides with a similarly expanding cloud from another star, at a time which is approximately $\tau = (n_* V_* \pi V_e^{\,2})^{-1/3}$, where n_* is the local density of stars losing mass and V_* is their r.m.s. random velocity component. From the mass distribution of equation (1.1), we expect $V_* \approx 200$ km s^{-1}. The density of stars undergoing mass loss depends on the length of time the stars are actively losing mass. If this phase takes the full lifetime of the star, $n_* \approx 10^3 (r_o/r)^2$ pc^{-3}. However, the period of active mass loss may be much shorter. Goldreich and Scoville (1976) suggest a typical mass loss rate of 3×10^{-5} $M_\odot$/yr. These values imply a range, $\tau = (10^3 - 10^5)(r/r_o)^{2/3}$ yrs. Through these inelastic

collisions the gas loses its random component and falls toward the galactic plane, forming a rotating gaseous disk. Such a disk is known to exist (see, for example, Oort, 1977).

High resolution radio observations (Balick and Sanders, 1974) indicate an ionized gas density of 10^4 cm^{-3} within 1 pc of the center. The observations of Pauls et al. (1975) imply that the density has fallen to about 10^2 cm^{-3} at a distance of 15 pc from the center along the plane of the galaxy. These values are consistent with the density dependence of the stars. The molecular line observations of CO by Sanders and Wrixon (1974) indicate that the quantity of neutral gas is about the same as the ionized gas at the center.

In sharp contrast to these distributions the results of Gatley et al. (1977) imply that the density distribution of dust is nearly uniform over the region within 15 pc of the center. This is an interesting result, since it is commonly believed that dust is formed either during or immediately after mass ejection from stars, and we should thus expect the gas to dust ratio to be constant. These authors suggest that some mechanism must either selectively destroy dust at, or push dust out of, the central region of the galaxy. Unless grains are composed almost entirely of ice (Wickramasinghe, 1965) the expected sputtering rate is too low for the first alternative to be acceptable. It is the second alternative, that dust grains may be pushed out of the galactic center, which is considered in this paper.

II. Conditions for Dust Flow

The radiation pressure on a dust grain is given approximately by the formula

$$F_r = \frac{F(r)\ \sigma\ q_{rp}}{c} \tag{1.3}$$

where $F(r)$ is the flux of radiation in ergs $cm^{-2}\ s^{-1}$, σ is the geometric cross section of a grain, q_{rp} is the ratio of the radiation pressure cross section to the geometric cross section, and c is the speed of light. The color temperature of the radiation field near the galactic center has been estimated to be about 4000 K (Van Den Bergh, 1965, cf. M31 as in Becklin and Neugebauer, 1968). Gilman (1974) has calculated the values of q_{rp} for a variety of materials and radiation color temperatures. For a color temperature of 4000 K, his results indicate the $q_{rp} \approx 1$ for grains larger than .1 μ and q_{rp} falls off approximately as$(r_g/.1\ \mu)$ for smaller grains. The ratio of the radiation force to the gravitational force is thus

$$\frac{Fr}{Fg} = \frac{3q_{rp}}{8\pi\ X\ c\ G\ r_g\ \rho_{gm}} \tag{1.4}$$

where X is the mass to luminosity ratio in solar units, r_g is the radius of the grain, G is the gravitational constant, and ρ_{gm} is the density of the grain material. The value of X has been estimated to be about 3 (Van Den Bergh, 1965) and choosing a value of 3 for ρ_{gm} we obtain

$$\frac{Fr}{Fg} \approx \begin{cases} 1 & r_{g5} < 1 \\ r_{g5}^{-1} & r_{g5} > 1 \end{cases} \qquad (1.5)$$

where r_{g5} is the grain radius in units of 10^{-5} cm. We see that the ratio probably never exceeds unity. However, the dust is immersed in gas. The opacity of the gas is much smaller than that for grains so the gas should experience a negligible radiation pressure, and thus is supported primarily by its rotation. The gas will stream past a dust grain which feels an effective dilute gravitational force (gravity + radiation pressure) and would naturally rotate at a much slower velocity than the gas. The angular momentum imparted to the grain from the gas then causes the grain to spiral outward. The same process will occur in a cloud that is in free fall. Notice that the Poynting-Robertson effect is negligible because the tangential force exerted by the gas on the grains has a magnitude approximately equal to the radiation pressure force, but the force due to the Poynting-Robertson effect is smaller by the factor $V/c \approx 10^{-3}$.

Crucial to this process is the drag that a grain experiences as it flows through gas. The drag on an uncharged grain for subsonic velocities is

$$\vec{F}_d = -4C_s \sigma \rho \vec{V}_r \qquad (1.6)$$

(Epstein, 1924), where C_s is the speed of sound, ρ is the density of the gas, and V_r is the velocity of a grain relative to the gas. As the grain

velocity is increased above the sound speed, the drag force takes the form

$$\vec{F}_d = -\rho \sigma |\vec{V}_r| \vec{V}_r \quad . \tag{1.7}$$

A continuous functional form is adopted by switching from the subsonic case to the "supersonic" case at $V = 4 C_s$.

Grains may be charged to several volts in H II regions (Moorwood and Feuerbacher, 1975; Simons, 1976). For a typical grain size this is about 10^3 electron charges per grain. Spitzer (1962) has calculated the drag on a charged particle as it passes through a plasma

$$\vec{F}_p = \frac{-\ell n \Lambda Z_g^2 \rho \vec{V}_r}{11.7 T^{3/2}} \text{ dynes} \tag{1.8}$$

where Λ is the plasma parameter, Z_g is the number of charges on the grain, and T is the temperature of the plasma. This law yields a much larger drag force than that for a neutral particle because of long range coulomb encounters. This effect is so great that we may consider the grains to be effectively frozen into the plasma of an H II region. Molecular line observations of CO (Sanders and Wrixon, 1974) indicate that comparable quantities of both neutral and ionized gas exist at the Galactic Center. We expect that H II regions are compact and temporary. Furthermore differential rotation and the high luminosity of H II regions should help dust negotiate a path around these viscous traps. Thus for

the purposes of calculating the drag we assume the gas to be neutral at a temperature of approximately 100 K. Note that for this approximation to be valid it is only necessary that the neutral gas be simply connected in a time averaged sense.

The effective drag may be increased by the presence of a galactic magnetic field. This will be discussed in section V.

III. The Structure and Formation of the Disk

To describe adequately the flow of dust grains near the galactic center we need some knowledge about the density and average velocity of the gas in which the dust is immersed. As mentioned in section I, the gas density falls off approximately as the square of the distance along the galactic plane, ω. Thus

$$\rho(\omega,z=0) = \rho_0(\frac{\omega_0}{\omega})^2 \tag{1.9}$$

where $\rho_0 = 10^{-20}$ gm/cm^3 and $\omega_0 = 1$ pc. The contribution of the mass in gas to the gravitational field produced by the stars is negligible, so the disk is not self gravitating. Under the assumption of constant thermal or turbulent velocity the z dependence of the density may be found from the hydrostatic equation which yields

$$\rho(\omega,z) = \rho_0(\frac{\omega_0}{\omega})^2 \exp(\frac{-Hz^2}{\omega^2}) \tag{1.10}$$

where $H = 4\pi G\rho_* {}^0r_0{}^2V_T{}^{-2}$ and V_T is the effective thermal or turbulent velocity of the gas. For a value of 10 km/sec, $H \approx 10$. This equation is only valid for $z^2/\omega^2 \ll 1$.

There are several effects which will cause the average gas velocity to deviate from purely Keplerian rotation.

The first, due to thermal or turbulent pressure, exists because the gas which is supported by this pressure will rotate at a velocity somewhat less than the Kepler velocity. The grains, which are much denser than the gas, will not be affected by the gas pressure gradient. However, they probably do feel the effect of a turbulent pressure, since they are coupled to this via viscous drag. This point is academic because the effect of either is insignificant. Consider the equation which balances the centrifugal, pressure, and gravitational forces on the gas along the galactic plane

$$\frac{V^2}{\omega} = \frac{1}{} \frac{dP}{d\omega} = g_{\omega} \quad , \tag{1.11}$$

where V is the rotational velocity, P is the pressure and g_{ω} is the gravitational acceleration along the plane toward the center. In the isothermal approximation we obtain the condition $V^2 = V_K^2 - C_S^2$ where V_K and C_S are the local Kepler and thermal or turbulent velocities, respectively. Since $C_S^2/V_K^2 < .01$, the gravitational and centrifugal forces differ by only 1% where the radiation force and the gravity force are about equal.

The second effect is due to magnetic torque which causes the gas to spiral inward. There may be a galactic magnetic field which is being amplified by differential rotation and turbulence. The magnitude of this field may not exceed the critical value $B_c = (8\pi\rho C_S^2)^{1/2}$ set by

the onset of instability (Parker, 1967). The inward velocity may be obtained by balancing the magnetic torque against the inward flux of angular momentum which yields $U = (C_S/V_K)C_S$. This may be compared to the grain velocities derived in Section V which are greater than C_S.

Finally, the ongoing formation of the disk will cause the gas within the disk to spiral inward. This is because the average rotational velocity, V, of the material falling on the disk is less than the Kepler value, V_K. We calculate this effect by solving the equations for the conservation of mass and angular momentum under the assumption of nearly circular orbits.

If U_d is the inward velocity of the gas, then the conservation of mass requires

$$\frac{\partial \rho}{\partial t} + \mathrm{Div}(\rho U_d) = \Gamma_D(\omega) \quad , \tag{1.12}$$

where ρ is the gas density, and $\Gamma_D(\omega)$ is the volume source function representing material falling onto the disk. This may be estimated by integrating the grain source function $\Gamma_g(\omega)$ of section I over a vertical path and dividing by an effective disk thickness at each ω, with the result

$$\Gamma_D(\omega) \approx 15\ \Gamma_o\left(\frac{\omega_o}{\omega}\right)^2 \quad , \tag{1.13}$$

where one density scale height (of equation (1.10)) has been used for the thickness of the disk.

The conservation of angular momentum can be expressed by the equation

$$\frac{\partial(\rho\omega V_K)}{\partial t} + \text{Div}\ (\rho U_d \omega V_K) = \Gamma_D(\omega)\ b\omega V_K \quad , \tag{1.14}$$

where b is the ratio V/V_K for material falling on the disk. Because the disk thickness is approximately proportional to ω, the appropriate form for the divergence is, Div $A = 1/\omega^2\ [d(\omega^2 A)/d\omega]$. Solving for the density and inward velocity along the plane, we obtain

$$\rho(\omega) = (2 - \frac{b}{3})\ \Gamma_D(\omega)\ t \quad , \tag{1.15}$$

$$U_d = (\frac{b - 1}{6 - b})\ (\frac{\omega}{t}) \quad . \tag{1.16}$$

The inward velocity depends on how long ago the disk started forming. This is due to the assumption that the function $\Gamma_D(\omega)$ is constant. The present observed disk density coupled with our estimate for the mass loss rate and equation (1.15) imply a disk age of about 2×10^7 yrs. The actual formation time could have been much earlier if the star formation rate nearly balances the mass loss rate. However, this is long enough so that the predicted inward velocities $U_d \approx .05\ \omega$ km/sec are small compared to the outward grain velocities derived in section V for the region within about 10 pc of the center. For the following calculations we assume that the gas has only a tangential component to the velocity of constant value $V_K \approx 200$ km/sec.

IV. The Flow of Dust through an Optically Thin Rotating Gaseous Disk

The details of the flow of grains depends on the ratio Fr/Fg, which may be uncertain by a factor of 10. The estimated value, near unity, will be lowered by the extinction of the radiation field (see section VI). We wish to discover what effect the variation of this ratio has on the details of the dust flow. In particular, under what conditions is the transfer of angular momentum from the gas to the dust so effective that the centrifugal and gravity forces balance so well that we may obtain the outward radial velocity of a grain by balancing only the radial drag against the outward radiation force.

The gravity is due to the mass distribution (cf. equation (1.1)). This distribution is fairly general, since any relaxed self-gravitating system without excessive angular momentum will have an approximately inverse square density distribution over most of its extent. The difference between the gravitational and centrifugal forces is given by $m_g/\omega\ (V^2(\omega) - V_K^2)$ where $V(\omega)$ is the tangential velocity and m_g is the mass of a grain. The balance of the radial forces on a grain thus yields

$$\vec{F}_d \cdot \hat{e}_\omega + \frac{m_g}{\omega}\,(V^2(\omega) - V_K^2) + |\vec{F}_r| = 0 \quad . \tag{1.17}$$

A second equation of motion is obtained by balancing the rate of change of angular momentum of the grain, against the tangential component of the drag force. Thus

$$\frac{dL}{dt} = m_g\{\omega(\frac{\partial V}{\partial t} + \frac{U dV}{d\omega}) + UV\} = \vec{F}_d \cdot \hat{e}_\theta \quad . \tag{1.18}$$

The tangential velocity of a grain should not deviate more than about 4 C_S from V_K because the drag law becomes "stiff" at supersonic velocities, so the first two terms on the left hand side have been neglected. The results are consistent with their omission. Using results from the preceding section, the equations are put in the dimensionless form

$$\alpha U V x = (V_K - V) \left\{ \begin{matrix} 4 \\ \tau \end{matrix} \right\} \quad , \tag{1.19}$$

$$\left\{ \begin{matrix} 4 \\ \tau \end{matrix} \right\} U = \alpha \left[\left(\frac{V^2(\omega)}{V_K^2} - 1 \right) + \beta \right] x \quad , \tag{1.20}$$

where the velocities are now mach numbers, $x = \omega/\omega_o$, $\tau = \sqrt{U^2 + (V - V_K)^2}$, $\alpha = \dfrac{m_g}{\sigma \rho_o \omega_o}$, and $\beta = Fr/Fg$. The constant α depends on the density, ρ_o, at the fiducial point, $x = 1$. For the galactic center $\alpha \approx 3 \times 10^{-3}$, $V_K \approx 200$, and $C_S \approx 1$ km/sec. Solutions of these equations, for $V_K = 200$, are displayed in Figure 1, for several values of α and β. The solutions show the radial mach number as a function of the radius in parsecs. All of the curves rise to a maximum and then fall toward zero. This behavior is a result of the radiation and gas density, distributions. The outward radial force is proportional to x^{-1}. The gas density, and therefore the drag coefficient, is proportional to x^{-2}. How effectively the angular momentum is transferred to the grains depends on this gaseous drag. Thus the transfer should be efficient for small enough values of x. For this regime, the gravitational and centrifugal forces should adequately balance, so the radiation and radial drag forces must be approximately equal. This implies that the radial grain velocity should

Figure 1a,b. This figure displays solutions of stationary grain flow through a rotating gaseous disk with density $\rho = \rho_o x^{-2}$. The gravitational field is inversely proportional to X, $g = V_K^2 X^{-1}$. The dimensionless radial grain velocity (Mach Number) is plotted against the dimensionless distance from the galactic center along the plane. The fiducial point, X = 1, is chosen to be 1 parsec, and the speed of sound, C_S, has been chosen to be 1 km/sec, so the figure may be read in km/sec for the velocity and parsecs for the distance. The dimensionless quantities α and β are $mg/\sigma\rho_o\omega_o$ and Fr/Fr, respectively. The parameter V_K = (rotation velocity/speed of sound) is fixed at 200 in Figure 1a, but is varied for Figure 1b while α and β are fixed at the values expected for the galactic center.

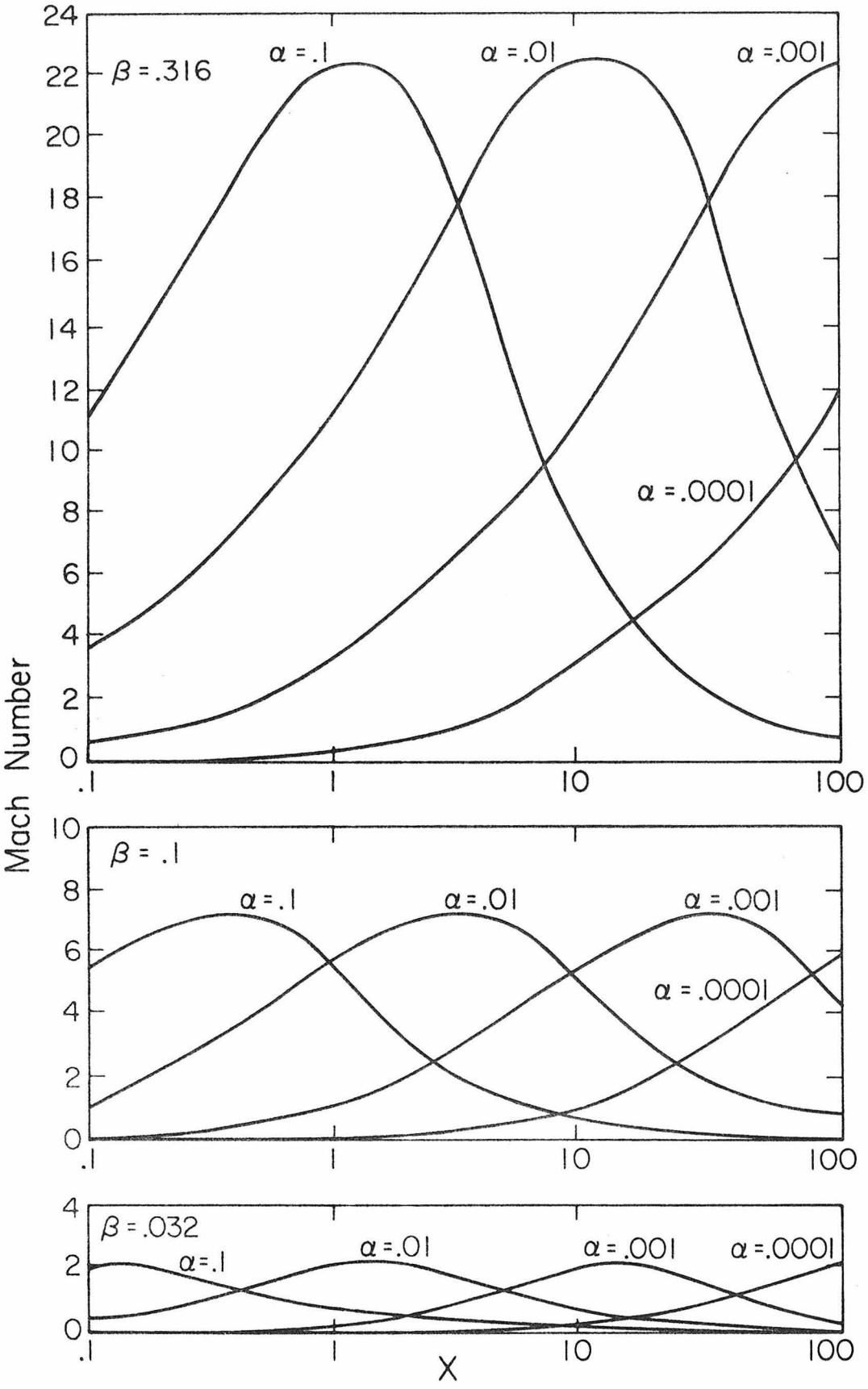
Mach Number
β = .316
α = .1
α = .01
α = .001
α = .0001
β = .1
α = .1
α = .01
α = .001
α = .0001
β = .032
α = .1
α = .01
α = .001
α = .0001
X

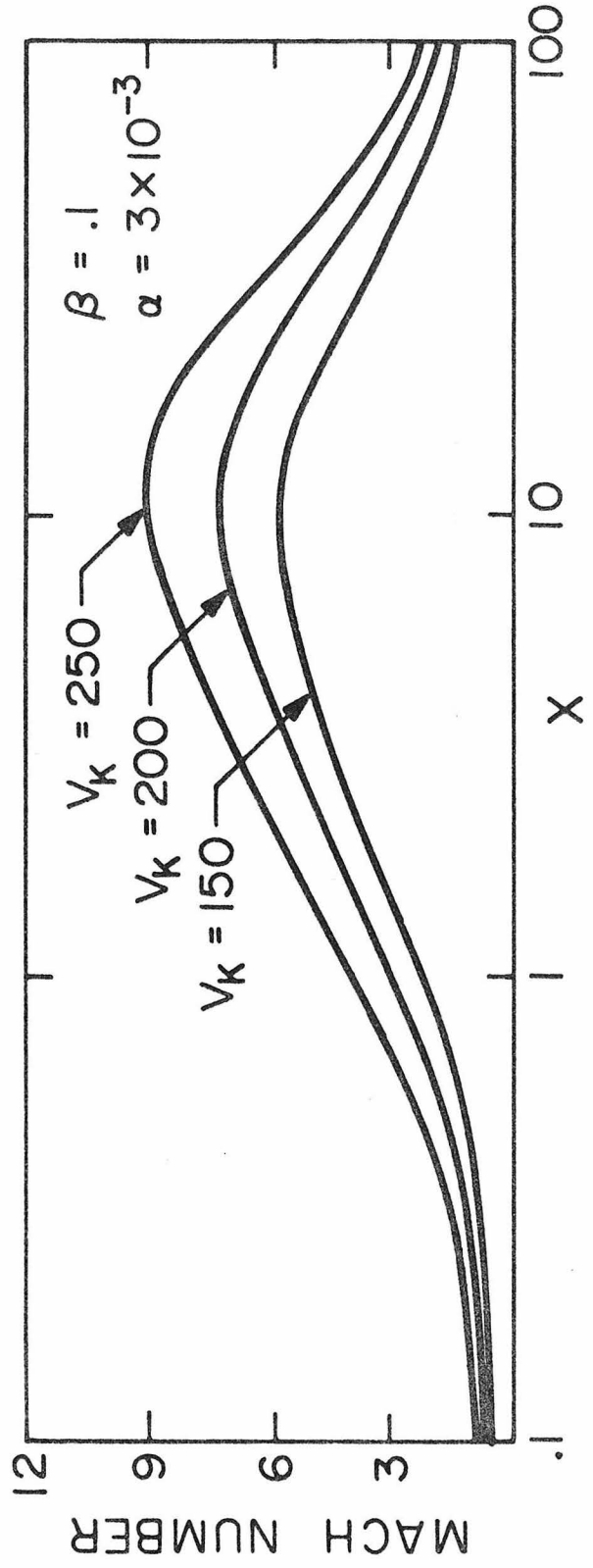
MACH NUMBER
12
9
6
3
.1
1
10
100
X
V_K = 250
V_K = 200
V_K = 150
β = .1
$\alpha = 3\times10^{-3}$

be proportional to X or $X^{1/2}$ depending on whether the grains have subsonic or supersonic velocities, respectively. With increasing x this approximation becomes progressively less valid. At some distance, X_c, the difference between the gravitational and centrifugal forces become important. The radial velocity of the grain becomes a decreasing function of X because the grains have to wait until the gas gives them enough angular momentum to continue outward. The value of X_c depends on α, V_K and β, where α and V_K are ratios of (gravity/drag) related constants and β = Fr/Fg (radiation/gravity). As α is increased the effect of drag decrease. Both β and V_K have a relatively small effect on X_c. Interestingly, the velocity at X_c does not seem to be a function of α (see Figure 1a,b). This is understandable because a decrease in α implies increased drag and hence the radius at which the gas is capable of delivering the grains' required angular momentum is increased. Furthermore, the necessary angular momentum transfer rate for constant outward grain velocity decreases as X^{-1}. Since the force due to radiation pressure is also proportional to X^{-1}, the velocity at X_c is not a function of α.

These results indicate that the transfer of angular momentum from the gas to the grains is so effective within about 10 pc from the galactic center that the radial velocity of grains is determined only by the balance of the radiation force against the radial drag component. This result will be used throughout the rest of this paper. In the next section we consider the effects of a magnetic field. From the dependence of X_c on α it is clear that an increase in the drag due to a magnetic field should increase the region over which this approximation is valid.

V. Galactic Magnetic Fields

A galactic magnetic field may affect the motion of dust grains since they might be charged. There are two competing effects which charge grains. First, since photons of energies greater than $\sim$ 10 ev can eject electrons via the photoelectric effect, they charge the grains positively. Second, the electron velocities are larger than the positive ion velocities and will bombard grains more frequently, charging the grains negatively. Grains can be charged to a positive potential of several volts near a source of ionizing radiation (Simons, 1976). Further away, some grains will become negatively charged. The distance depends on the composition and size of the grain. Far enough away the charge on all grains should be negative. Since the coulomb drag is excessive for a grain charged to several volts in an H II region (cf. equation (1.8)) we are only interested in grains immersed in neutral gas. However, even H I regions are ionized to some degree and so the grains may have a small negative charge. Watson (1972) calculates grain potentials of several tenths of a volt. The charge on a grain may be expressed by the formula

$$q = 3 \times 10^{-8} \, r_{g5} \, \phi \text{ esu} \tag{1.21}$$

where r_{g5} is the grain radius in 10^{-5} cm, and ϕ is the potential in volts.

No direct measurement of the magnetic field in the galactic center has been made, but differential rotation may have amplified whatever seed field existed at disk formation. An upper limit may be placed on the magnetic field because a clumping instability sets in when

the magnetic energy density $B^2/8\pi$ is equal to the gas thermal energy ρC_S^2 (Parker, 1967). (The magnetic field floats out of the gas due to its buoyancy.) We assume that the galactic magnetic field is some fraction ξ of this critical field. The orientation of the magnetic field is probably randomized by turbulence (i.e., cloud motions in the gas). A simple treatment to calculate the effect of this magnetic field on the motion of a grain is presented. We follow the motion of the guiding center so we must be sure that the cyclotron radius is small compared to the thickness of the disk. The cyclotron radius is

$$|\vec{r}_c| = |\frac{c}{qB^2}(\vec{P} \times \vec{B})| \approx 10^{13}\ \rho_{gm}\ r_{g5}^2\ M\ \xi^{-1}\ \phi^{-1}\ \text{cm} \quad , \tag{1.22}$$

where M is the speed in km s^{-1} (mach number) and ρ_{gm} is the grain density. The disk thickness is thus much greater than V_c for all reasonable parameters. We can then calculate the drift velocity of the guiding center from the formula

$$\vec{V}_d = \frac{c}{qB^2}(\vec{f}_r + \vec{f}_{\nabla B}) \times \vec{B} \tag{1.23}$$

(Alfvén and Fälthammer, 1963), where the body force $\vec{f}_r$ is the vector sum of the gravitational, centrifugal, radiation pressure, and drag forces, and $f_{\nabla B} = (P^2/2M)(\nabla B/B)$, where P is the momentum of the grain perpendicular to the magnetic field. The force due to $\vec{f}_{\nabla B}$ may be enhanced on small scales due to the turbulent nature of the field. However, we are interested in the average large scale motion of the grains. The limit

on the magnetic field $B_c = \sqrt{8\pi\rho C_s^2}$ coupled with the density dependence of the gas can be used to estimate this force. The result is smaller than the radiation pressure force by about a factor of 10,000 and may be neglected.

For the central regions (see section IV) the gravitation and centrifugal forces balance. Thus $\vec{f}_r$ consists of the radiation force $\vec{F}_r$ and the viscous drag $\vec{F}_d$. Only the component of $\vec{B}$ perpendicular to the $(\vec{F}_r,\vec{F}_d)$ plane has any effect on the grains' motion. Therefore without loss of generality we set up the orthogonal vector triad $(\hat{e}_1,\hat{e}_2,\hat{e}_3)$ and fix $\vec{F}_d$ parallel to $\hat{e}_1$, $\vec{B}$ parallel to $\hat{e}_3$, and $\vec{F}_r$ within the $(\hat{e}_1,\hat{e}_2)$ plane. Decomposing $F_r = F_1\hat{e}_1 + F_2\hat{e}_2$ and substituting into equation (1.23) we obtain

$$V_d\hat{e}_1 = \frac{c}{qB^2}\left[F_1\hat{e}_1 + F_2\hat{e}_2 - |F_d|\,\hat{e}_1\right] \times B\hat{e}_3 \tag{1.24}$$

where F_d is taken to be the average drag force over a cyclotron orbit, $F_d = 4C_s\sigma\, V_d$ for subsonic velocities and $F_d = \sigma V_d^2$ for supersonic velocities. Self consistency requires

$$F_r \cos\theta = \begin{cases} 4C_s\sigma\rho V_d & \text{subsonic} \\ \rho\sigma V_d^2 & \text{supersonic} \end{cases} \tag{1.25}$$

$$V_d = \frac{c|F_r|}{qB}\sin\theta \tag{1.26}$$

This approximation is valid when the Lorentz force is large compared to the drag force. Using the approximation $\sin\theta \approx 1$ we obtain

$$V_d \approx \frac{CF}{qB} \tag{1.27}$$

and

$$\cos\theta = \begin{cases} \dfrac{4C_S\sigma\rho c}{qB} & \text{subsonic} \\ \\ \dfrac{\rho\sigma c^2 F}{q^2B^2} & \text{supersonic} \end{cases} . \tag{1.28}$$

Since the magnetic field is randomly oriented the velocity component which is perpendicular to the applied force will be averaged out. We are thus interested in the component which is parallel to $\vec{F}$

$$V_{||} = \begin{cases} \dfrac{4F\rho C_S\sigma c^2}{q^2B^2} \simeq 2 \times 10^{23}\ C_{S5}^{-1}\ (\phi\xi)^{-2}\ F\ cm^{-1} \\ \\ \dfrac{F^2c^3\rho\sigma}{q^3B^3} \approx 2.5 \times 10^{38}\ (\phi\xi C_{S5})^{-3}\ r_{g5}^{-1}\ F^2\ \rho_{-20}^{1/2} \end{cases} , \tag{1.29}$$

where C_{S5} is the speed of sound in units of 10^5 cm^{-1}, ρ_{-20} is the density of the gas in units of 10^{-20} gm cm^{-3}, F is in dynes, and $V_{||}$ is in cm s^{-1}. The drag law switches from the subsonic to the supersonic form at the critical force

$$F_c = 2 \times 10^{-17} \phi\, r_{g5}\, \rho_{-20}^{1/2}\, C_{S5}^2 \text{ dynes} \quad . \tag{1.30}$$

With increased force the ratio of the Lorentz force over the viscous drag force decreases until it is appropriate to neglect the magnetic field. The magnetic drag relation is depicted schematically in Figure 2.

The force near the galactic center is not sufficient to produce supersonic flow of grains. Using the first relation along with the results of the preceding sections we obtain the radial drift velocity of grains near the center,

$$V_r = 2 \times 10^5\, C_{S5}^{-1}\, (\phi\xi)^{-2}\, (r_o/r)\, \beta \text{ cm/sec} \quad . \tag{1.31}$$

We now estimate the distribution of grains from the continuity equation:

$$\frac{1}{r^2} \frac{d}{dr} (r^2 \rho v) = \Lambda_g(r) \quad , \tag{1.32}$$

which yields a constant density distribution of grains

$$\rho_g = 1.5 \times 10^{-24}\, C_{S5}\, (\phi\xi)^2\, (Fr/Fg)^{-1}\, \Lambda_{g-37} \text{ gm cm}^{-3} \tag{1.33}$$

where we have assumed a source function for grains $\Lambda_g(r) = \Lambda_{g-37}^o\, (r_o/r)^2$ where Λ_{g-37} is in units of 10^{-37} gm s^{-1} cm^{-3}. The observations of Gatley et al. (1977) indicate a uniform grain density of 3×10^{-24} gm cm^{-3}. Agreement is obtained for a reasonable choice of parameters, e.g., $\xi = 1$, $\phi = .4$, and $Fr/Fg = .1$.

Figure 2. This figure schematically displays the effect of a turbulent magnetic field on the drag force versus velocity relation of a charged grain. Curve A is the relation for the case of no magnetic field. F_c is the force which produces supersonic grain motion, i.e., $|\vec{V}_d| \geq 4C_S$. $\vec{V}_d$ is the velocity of the grain through the gas. For the case of no magnetic field this is parallel to the force thus $\vec{V}_d = \vec{V}_{||}$. Curve B displays the $\vec{V}_{||}$ vs. force relation for gas plus a turbulent magnetic field. Because of the Lorentz force $|\vec{V}_{||}| < |\vec{V}_d|$. For $F > F_c$ the gaseous drag is proportional to V_d^2 but the Lorentz force is proportional to V_d; Thus the drag relations meet at some critical force, F_L.

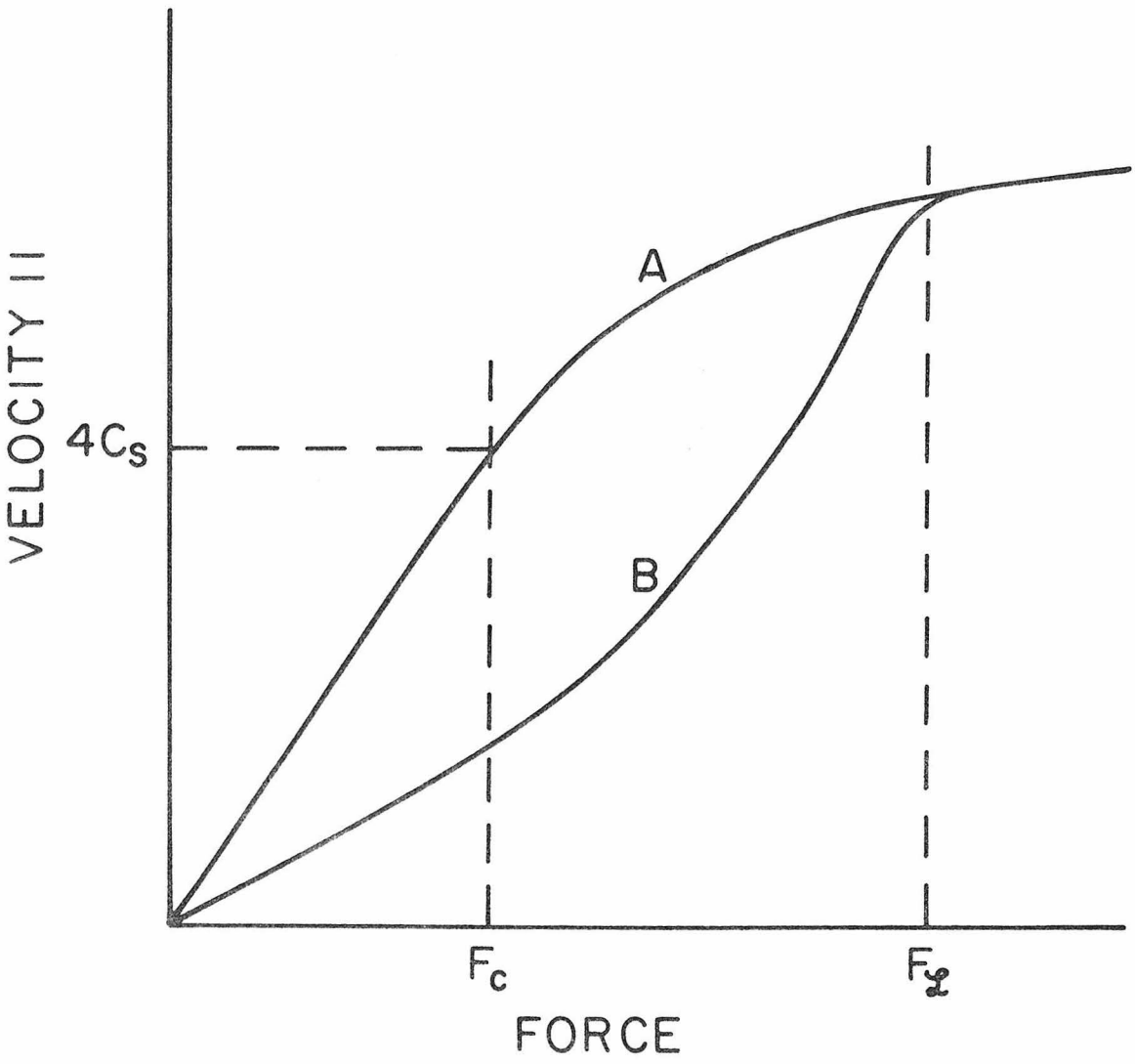
VELOCITY II
$4C_s$
A
B
F_c
F_{ℓ}
FORCE

VI. Extinction

We have estimated the ratio of Fr/Fg to be near unity under the assumption of no extinction. An estimate of the extinction at the peak of the black body spectrum (0.7 μ) of 0.14 magnitudes per parsec has been made by Gatley et al. (1977). Therefore, we expect the ratio Fr/Fg to drop by a factor of 10 at a distance of 15 pcs from the center. The ratio should actually not drop this much because the optical depth of the disk in the z direction is probably never greater than unity, within 15 pcs from the center. This range in Fr/Fg is consistent with the needs of the preceding sections.

VII. The Stability of Radiation Driven Dust Flows

The results of the preceding sections indicate that the dust near the galactic center should have a nearly uniform distribution. By analyzing the stability of the dust flows we determine if this distribution is uniform on small scales (i.e., is the dust clumpy?). The formation of local dust to gas density enhancements may contribute to the formation of dark clouds and thus ultimately be important to the understanding of star formation. To simplify the stability analysis an initially uniform distribution of stars, gas and dust is assumed, and the equations are written in slab geometry. The radiative transfer is handled using the forward-reverse approximation (see Zel'dovich and Raizer, 1967). The gas velocity is taken to be zero everywhere and is important only through its drag on the grains. The velocity of the grains is given by the formula

$$V_g(x,t) = C_d\, F(x,t) \quad , \tag{1.34}$$

where the constant C_d adsorbs the drag law and the radiation pressure cross section of a grain, and $F(x,t)$ is the radiation flux. The conservation of grains requires

$$\frac{\partial \rho_g(x,t)}{\partial t} + \frac{\partial}{\partial x}\left(\rho_g(x,t)\, V_g(x,t)\right) = \Lambda_g(x) \tag{1.35}$$

and the radiative transfer equations are written in the form

$$\frac{\partial I_+(x,t)}{\partial x} = \frac{S}{2} - K\, \rho_g(x,t)\, I_+(x,t) \quad , \tag{1.36}$$

$$\frac{\partial I_-(x,t)}{\partial x} = -\frac{S}{2} + K\, \rho_g(x,t)\, I_-(x,t) \quad , \tag{1.37}$$

$$F(x,t) = I_+(x,t) - I_-(x,t) \quad , \tag{1.38}$$

where $I_+(x,t)$ and $I_-(x,t)$ are the outgoing and ingoing radiation fluxes, respectively. S is a source function which represents the average luminosity/cm^3 of the stellar distribution. Equations (1.32-1.35) are linearized and solutions of the form $e^{+i(\tilde{K}x - \tilde{\omega}t)}$ are sought. The resulting dispersion relation is

$$\tilde{\omega} = i\, \frac{C_d S}{1+\Lambda_K^2} \tag{1.39}$$

where $\Lambda_K = \rho_o K/\tilde{K}$, for ρ_o is the initial grain density, and $\tilde{K}$ is the wave-number of the perturbation. Thus perturbations are strongly unstable for scale sizes smaller than $(k\rho_o)^{-1}$ which is about 6 pc near the galactic center. Using values from the preceding sections to determine C_d and S, the growth time for the perturbations is found to be approximately

$$\tau \approx 2 \times 10^5 \, C_{S5} \, (\frac{\phi\xi}{r_{g5}})^2 \, (r/r_o)^2 \text{ yrs} \quad . \tag{1.40}$$

Astronomically this is an exceedingly short time. Turbulent motions and differential rotations must increase this time but by how much is uncertain. Notice that the predicted time scale is shorter than the age of the galaxy even 1 kpc from the center if ϕ is as small as 0.3, which is not unreasonable. It seems likely that this mechanism is important for the formation of dark clouds.

VIII. Conclusions

Grains may be driven out of stellar systems by radiation pressure even when this force does not exceed the opposing gravitational force if there is a rotating gaseous disk. The disk is necessary to give grains angular momentum which allows them to spiral outward. This situation probably exists at the galactic center.

The flow of grains through H II regions is not important because of the large coulomb drag.

A galactic magnetic field can significantly affect the drag on a grain even in an H I region. The effect has been calculated for the galactic center and a uniform density distribution of grains results.

This is in agreement with the observations and inferences of Gatley et al. (1977).

Finally, the flow of dust grains driven by radiation pressure is unstable. Grains tend to clump producing local enhancements in the dust to gas ratio. The time scale for clumping has been estimated to be about 2×10^4 y near the galactic center. The timescale increases with distance from the center because the radiation intensity decreases, but may still be smaller than the age of the galaxy at distances up to a Kpc. This mechanism could be partly responsible for the formation of dark clouds.

Acknowledgements

I am particularly grateful to Ian Gatley who suggested that I work on this problem and spent many helpful hours discussing various observations of the galactic center. I would like to thank my advisor, James E. Gunn, for encouragement and helpful suggestions. I would also like to thank Vincent Icke, Eric Persson, Steven Beckwith, and an anonymous referee for helpful criticisms of the manuscript. This work was supported by the National Science Foundation under AST76-80801.

References

Alfvén, H. and Fälthammer, C., 1963, Cosmical Electrodynamics (Oxford: Clarendon Press).

Balick, B. and Sanders, R. H., 1974, Ap. J. 192, 325.

Barlow, M. J., 1971, Nature Phys. Sci., 232, 152.

Becklin, E. E. and Neugebauer, G., 1968, Ap. J. 151, 145.

Epstein, P. S., 1924, Phys. Rev., 23, 710.

Gatley, I., Becklin, E. E., Werner, M. W., and Wynn-Williams, C. G., 1977, Ap. J.,

Gilman, R. C., 1974, Ap. J. Suppl. 28, 397.

Goldreich, P. and Scoville, N., 1976, Ap. J., 205, 144.

Moorwood, A. F. M. and Feuerbacher, B., 1975, Ap. Space Sci., 34, 137.

Oort, J., 1977, Ann. Rev. Astr. Ap., 15, 295.

Parker, E. N., 1967, Ap. J., 149, 517.

Pauls, T., Downes, D., Mezger, P. G. and Churchwell, E., 1976, Astr. Ap., 46, 407.

Sanders, R. H. and Lowinger, T., 1972, A.J., 77, 292.

Sanders, R. H. and Wrixon, G. T., 1974, Astron. Astrophys. 33, 9.

Simons, S., 1976, Ap. Space Sci., 41, 423.

Spitzer, L., 1962, Physics of Fully Ionized Gases (New York: Interscience), 2nd ed.

Touloukian, Y. S., 1967, Thermophysical Properties of High Temperature Solid Materials (New York: Macmillan).

Van den Bergh, S., 1965, A.J., 70, 124

Watson, W. D., 1972, Ap. J., 176, 103.

Wehner, G. K., 1957, Phys. Rev., 108, 35.

Wickramasinghe, N. C., 1965, M.N.R.A.S., 131, 177.

Zel'dovich, Y. B. and Raizer, Y. P., 1967, Physics of Shock Waves and High Temperature Hydrodynamic Phenomena (New York: Academic Press).

Chapter 2

On the Acceleration of Shock Waves in the Atmospheres of Cool Mira Variable Giants

Abstract

The velocity of shock waves in the photosphere of Mira variables can be observed through emission lines. These velocities are typically 5-10 km s^{-1}, which is less than their escape velocities, which are 20-40 km s^{-1}. This paper considers the propagation of these shocks outward from the photosphere, in particular the question of whether these shocks accelerate to a velocity that is sufficient to eject matter. It is found that shocks do accelerate, but not indefinitely. They reach a terminal velocity which is a function of the initial conditions of the gas (the fraction of hydrogen in its molecular state). For cool stars ($T \lesssim 2400$ K) nearly all hydrogen is in its molecular form and the terminal velocity is approximately 25 km s^{-1}. The velocity jump across the shock is approximately three-fourths of the propagation velocity, or about 20 km s^{-1}. For stars with escape velocities less than 20 km s^{-1} the shocks should eject a shell of matter once each stellar pulsation period. For hotter stars the terminal velocity will be correspondingly less, and therefore this mechanism should only be important for very cool stars with low escape velocities, the type of stars that are known to have high mass loss rates.

I. Introduction

Late M spectral type Mira stars are known to be losing a significant amount of mass, which appears in the form of a dust shell surrounding these stars. Some of the stars also have maser emissions associated with them (OH/IR stars) which indicates that the ejected matter has a velocity of approximately 20 km s^{-1}. One mechanism which could be responsible for this mass loss is based on grains formed in the star's cool atmosphere ($T \lesssim 2400$ K) which are then driven off by radiation pressure, dragging along the gas to which they are momentum-coupled by collisions (Gehrz and Woolf, 1971).

A lunar occultation measurement of IRC + 10011 has been made by Zappala et al. (1974). These results indicate that the region within three stellar radii of this star has a much lower opacity than the surrounding shell, implying that grains might not be forming that close to the star. This implies that alternate mechanism may be responsible for ejecting mass from the stellar photosphere, although radiation pressure on grains may still be important farther out from the star.

That shocks may be the cause of this mass ejection is not a new suggestion (Deutsch, 1960). However, this paper will not try to deal with the general problem of shock formation in the stellar envelope, but will narrow its attention to one very specific question. Given the observed shock velocities in the stellar photosphere of 5-10 km s^{-1}, can these shocks accelerate to velocities sufficient to eject matter as they propagate outward from the photosphere through a negative density gradient?

A spherical shock wave encompassing the star is formed each time the star is in its expanding phase. This shock wave is formed because the pulsation velocity which is subsonic deep in the star's envelope is supersonic in the much cooler atmosphere. The hot envelope, acting as a spherical piston, drives a shock through the stellar atmosphere.

Shock waves speed up when travelling down density gradients or through channels of decreasing area. In the atmospheres of Mira variables the shock waves travel down a density gradient, but are spherically diverging, and thus increase in area. However, because the atmospheric density scale height is smaller than the radius by a factor of nearly 100, and the shock velocity depends only weakly on an increase in area (if at all),[1] the small effects due to sphericity can be ignored (plane-parallel approximation); thus we expect that in the absence of damping the shock waves will speed up.

In §§ 2-5, a solution will be developed that includes the effects of dissociation but neglects radiation losses. The Mach number as a function of density is plotted in Figure 3 for the two cases, (1) without dissociation, and (2) with dissociation. In both cases the shock velocity increases monotonically with decreasing density, although more slowly in case 2.

In § VI it will be shown that radiation losses are unimportant for small Mach numbers, but become very large at a Mach number of approximately 7. This sudden increase occurs at a velocity that is just

---

[1]Similarity solutions exist for an expanding spherical piston moving at constant velocity in a uniform density gas. A shock wave is formed which has a constant velocity as it expands (Taylor, 1946).

sufficient to totally dissociate the H_2 molecule. For faster velocities the postshock energy (thermal) goes into radiation-producing mechanisms. Thus the solution produced in §§ 2-5 will be valid up to this velocity and it is clear that the shock will not accelerate past this terminal velocity (§ VI).

The minimum velocity sufficient to dissociate all of the H_2 molecules depends on the initial fraction of H_2 relative to H. For temperatures $\leq$ 2400 K nearly all hydrogen is in its molecular form, and this velocity is approximately 25 km s^{-1}. For hotter stars the fraction of H_2 is less and thus the terminal velocity is less also. Therefore this mechanism can only be important for very cool stars with small escape velocities.

II. Formulation of the Problem

We need to follow the motion of the shock wave through several (< 10) density scale heights, which the shock will traverse in a time much smaller than the stellar period. Therefore we can make the approximation that the photosphere moves with constant velocity during the expansive phase of the stellar pulsation. After the shock has reached its terminal velocity it will propagate at constant velocity until the star recontracts and sends out a rarefaction wave that will catch up to and dissipate the shock wave. This occurs after the shock has gone about one stellar radius.

The complicated details of opacity due to H_2O, H^-, CO, etc., that are important in a detailed model atmosphere will be used only in

the sense that the original density configuration will be taken from such a model. For the shock structure itself we will assume that the thermodynamic properties of the gas are dominated by molecular and atomic hydrogen.

Solutions for shock waves travelling through a density gradient exist in the literature. These solutions deal with radiationless, chemically inert, ideal gases, and therefore must be generalized for our problem. For late-type Mira variables the atmospheric temperatures are low enough that hydrogen exists mostly in its molecular state. This implies that there will be a dissociative relaxation zone behind the compression front of the shock.

The effects of dissociation will be put directly into the calculation. The results are displayed in Figure 3. The effects of radiation losses will be handled separately in § VI.

III. The Shock Structure

The structure of a shock wave propagating through a molecular gas may be conveniently separated into four regions (Fig. 1). The first region is the initial undisturbed gas. This state is not always completely undisturbed, but could be affected by precursor radiation; however, as long as the shock velocity is insufficient to totally dissociate the hydrogen molecules, the final state of the gas will be relatively cool and precursors will remain unimportant. The second is a compression front which has a thickness of from 10-100 meters. Only the fastest reactions occur in this region. These reactions are the excitation of the translational, rotational and vibrational degrees of freedom, which can be

Figure 1. This figure schematically represents the structure of a shock with a relaxation zone. The shock is moving to the right. Region 1 is the initial undisturbed gas. Region 2 is the compression front. Region 3 is the relaxation zone, and region 4 is the postshock zone where H_2 has come to dissociative equilibrium.

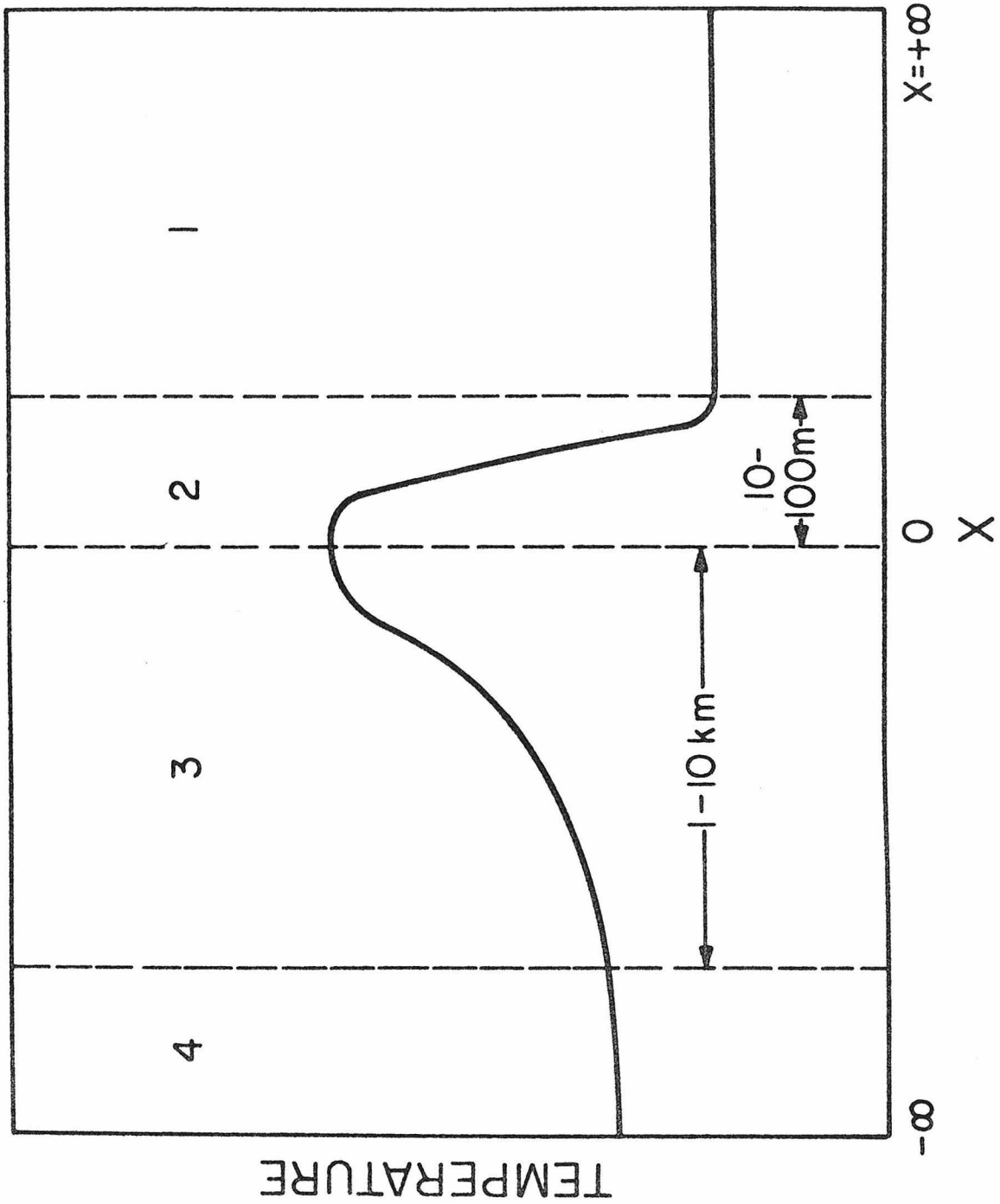

Fig. 1

accounted for by using an effective γ of 9/7. The third region is a relaxation zone where slower reactions occur, e.g., the dissociation of the hydrogen molecule. Radiative cooling competes with this reaction. I have investigated radiation from the rotational and vibrational lines of H_2 and H_2O, and from the excitation of elements ($z > 2$) by both neutral particle collisions and electron collisions. I found that dissociation is much faster than these processes and therefore they can be ignored (see § VI). Therefore the thickness of this region will be determined by the dissociation rate of the H_2 molecule. This thickness is approximately 10 km. The fourth region will be called the postshock zone. This is all of the gas, after the shock has passed, which has come to dissociative equilibrium, but is still a temperature where radiation losses may be important. It is from this zone that the shock can lose significant energy. How much will depend on the final state that the gas is left in, i.e., its temperature, degree of excitation, etc.

IV. The Relaxation Zone

I will not calculate the detailed structure of the relaxation zone, which would require the kinetic equations, because it is not necessary for this problem. Some simple and general results can be obtained by looking at the integral forms of the fluid equations.

$$\rho(x)\, u(x) = \rho' u' = \rho_0 u_0 \quad , \tag{2.1}$$

$$P(x) + \rho(x)\, u(x)^2 = P' + \rho' u'^2 = P_0 + \rho_0 u_0^2 \quad , \tag{2.2}$$

$$h(x) + \frac{u(x)^2}{2} = h' + \frac{u'^2}{2} = h_0 + \frac{u_0^2}{2} \quad , \tag{2.3}$$

where ρ = density, P = pressure, h = enthalpy, and u = velocity. The variables with subscript zero are the density, pressure, etc., for the undisturbed gas (region 1, Fig. 1), the primed variables correspond to the state of the gas just after the compression front, and the variables that are a function of position respresent the relaxation zone (region 3, Fig. 1). As $x \to \infty$ these variables reach their equilibrium values (region 4, Fig. 1). The enthalpy change remains small through the dissociation zone (Zel'dovich and Raizer, 1967). This is because the rate of dissociation is too small to establish large pressure gradients due to the increased speed of sound after the compression front. Therefore $u(x) \approx u'$ and from equation (2.3) we see that the enthalpy must also be nearly constant. The assumption of nearly constant enthalpy may be used to calculate the final dissociation fraction as a function of shock velocity. For the enthalpy we have $h = \varepsilon + P/\rho$, with

$$\varepsilon = \frac{7}{2}(1 - \alpha)RT - 2\alpha\frac{3}{2}RT + \alpha E = (\frac{7}{2} - \frac{\alpha}{2})RT + \alpha E \quad , \tag{2.4}$$

where E is the dissociation energy. Combining these we get

$$h = (\frac{9}{2} + \frac{\alpha}{2})RT + \alpha E = \frac{9}{2}RT' \quad . \tag{2.5}$$

Solving for α neglecting $\alpha/2$ compared with 9/2 we obtain

$$\alpha = \frac{9}{2}\frac{T' - T}{T_d} \quad , \tag{2.6}$$

where $T_d = E/R$. We need another relation to solve for α and T. The relation is the equation for dissociation equilibrium analogous to the Saha equation for ionization equilibrium,

$$\frac{\alpha^2}{1-\alpha} = \frac{K(T)}{4N} \quad ; \tag{2.7}$$

$$K(T) = \frac{M_H \nu}{I_{H_2}} \left(\frac{M_H}{\pi KT}\right)^{1/2} \frac{g_H^2}{g_{H_2}} \exp\left(-\frac{T_d}{T}\right) \quad ,$$

where M_H is the mass of the hydrogen atom, I_{H_2} is the moment of inertia for the H_2, ν is the vibrational frequency, and g_H and g_{H_2} are the degeneracy of the H atom and H_2 molecule, respectively. From equations (2.6) and (2.7) we get a transcendental equation which has been solved with the results plotted in Figure 2, along with the results for hydrogen ionization.

The temperatures after the compression front, after the dissociation of the H_2 molecule, and after the ionization of the hydrogen atom are plotted against velocity. The fraction of H_2 molecules and the fraction of ionized hydrogen atoms are also plotted. The temperature and degree of ionization were calculated assuming the gas to be thin to continuum radiation.

V. Solutions

I have used a formalism developed by G. B. Whitham (1958) to solve for the functional dependence of the shock velocity on density. Whitham has used his method to calculate this dependence in a plane-parallel

Figure 2. The results of § IV are plotted against velocity and the temperature directly after the compression front (region 2 in Fig. 1). Curve 1 is the final temperature for a shock with no relaxation zone. Curve 2 is the final temperature after the H_2 molecule comes to dissociative equilibrium. Curve 3 is the temperature after the H atom has come to ionization equilibrium. The curve labeled α is the fraction of dissociated H_2 molecules, and β is the fraction of ionized H atoms. Initial temperature was 2000 K.

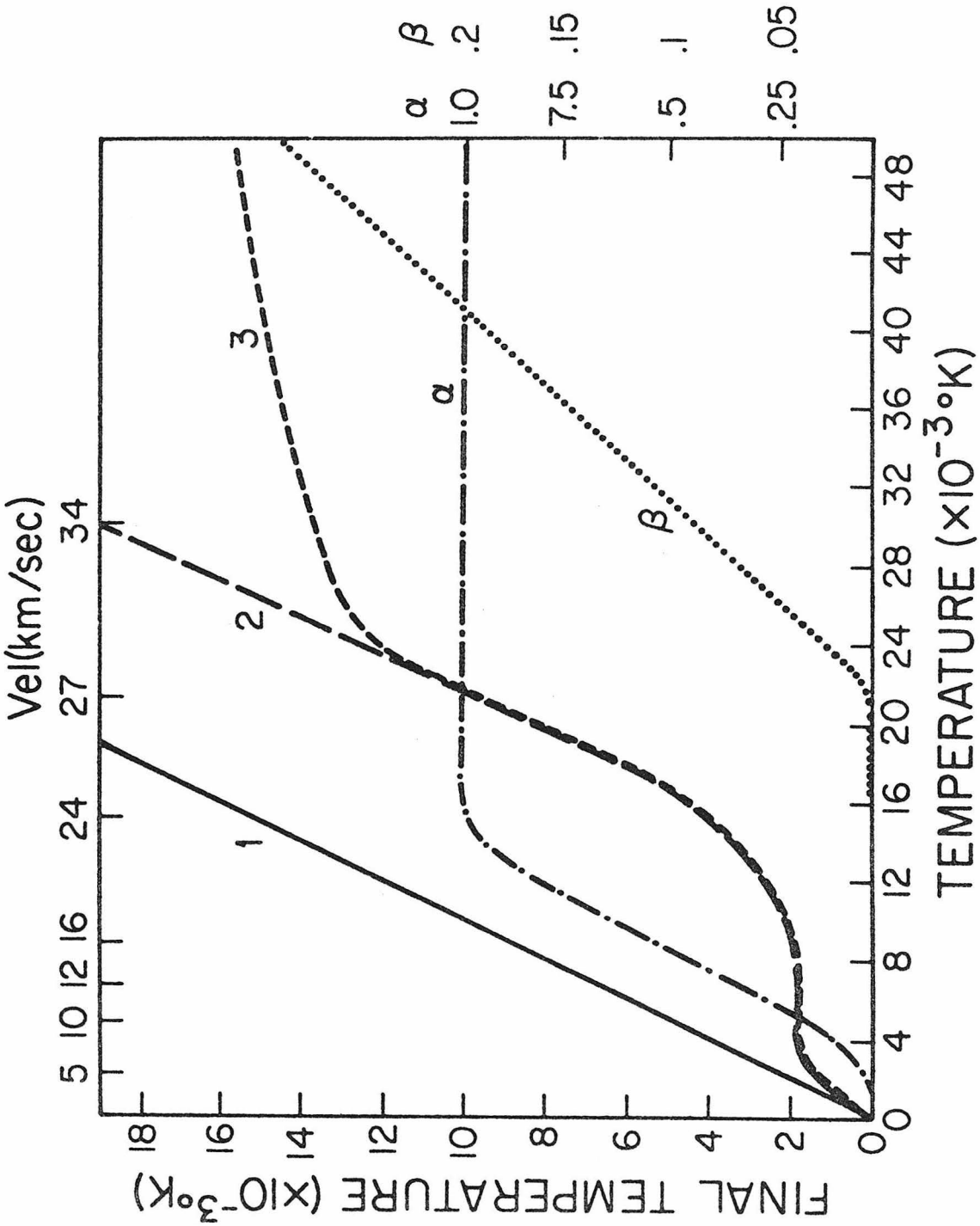
FINAL TEMPERATURE (X10⁻³°K)
TEMPERATURE (X10⁻³°K)
Vel(km/sec)
α
β
1
2
3

Fig. 2

ideal gas and found the following solution in the limit of very strong shocks:

$$M \propto p_0(x)^{-\beta} \qquad P \propto p_0(x)^{1-2\beta} \quad , \tag{2.8}$$

where

$$\beta = \{2 + [2\gamma/(\gamma - 1)]^{1/2}\}^{-1} \quad .$$

Whitham's method consists of the following procedure. The equations of motion must be written in characteristic form. The equations of motion are

$$\rho_t + u\rho_x + \rho u_x = 0 \quad , \tag{2.9}$$

$$u_t + uu_x + \frac{P_x}{\rho} = g \quad , \tag{2.10}$$

$$P_t + uP_x - a^2(\rho_t + u\rho_x) = 0 \quad , \tag{2.11}$$

where a is the speed of sound and u is the velocity of the gas. The initial undisturbed state is described by

$$P = P_0(x) \quad , \qquad \rho = \rho_0(x) \quad , \tag{2.12}$$

where

$$\frac{1}{\rho_0}\frac{dP_0}{dx} = g \quad .$$

The forward characteristic equation of motion is found by multiplying equation (2.10) by $\rho a/(u + a)$, using equation (2.9) to

substitute for ρ_t, multiplying equation (2.11) by $1/(u + a)$, and then adding. We get

$$\left(\frac{P_t}{u + a} + P_x\right) + \rho a\left(\frac{u_t}{u + a} + u_x\right) - \frac{\rho a}{u + a} g = 0 \quad , \tag{2.13}$$

or

$$dP + \rho a du - \frac{\rho a}{u + a} g = 0 \quad .$$

The final step is to plug the shock relations into this equation and solve the resulting first-order differential equation. In general this involves numerical integration, but for strong shocks the third term can be ignored and the solution is easily found.

This procedure can be used for a gas where dissociation is important by using the appropriate shock relations. The shock relations are derived from the equations

$$[\rho u] = 0 \quad , \qquad [P + \rho u^2] = 0 \quad , \quad \left[h + \frac{u^2}{2}\right] = 0 \quad , \tag{2.14}$$

where the brackets mean difference in these variables in front of and behind the shock.

The thermodynamics of the gas enters through the equation of state and the functional dependence of the enthalpy. For an ideal gas these are $P = \rho RT$ and $h = P/[(\gamma - 1)\rho] + P/\rho$. For a dissociating diatomic gas they are $P = (1 + \alpha)\rho RT$ and $h = (7 - \alpha) + P/[2\rho(1 + \alpha)] + \alpha E + P/\rho$, where α is the fraction of molecules dissociated. Using these relations, I found the shock relations to be

$$P = \frac{7}{18}\rho_0 a_0^2 F \quad , \tag{2.15}$$

$$\rho = \frac{28}{9}\frac{\rho_0 a_0^2 F}{1+\alpha_1}\left[2(\alpha_0 - \alpha_1)E + \frac{7}{9}a_0^2\left(\frac{8}{1+\alpha_0} + \frac{1}{2}F\right)\right]^{-1} \quad , \tag{2.16}$$

$$u = a_0\left[M - \left(\frac{16 + F}{12F^{1/2}}\right)\right] \quad , \tag{2.17}$$

where

$$F = \frac{9}{7}\left\{\frac{7 - \alpha_1}{8}M^2 + \left[\left(\frac{7 - \alpha_1}{8}M^2\right)^2 + \frac{\alpha_1 - \alpha_0}{a_0^2}(1 + \alpha_1)EM^2\right]^{1/2}\right\} , \tag{2.18}$$

M is the Mach number of the shock wave velocity, and α_0 and α_1 are the fraction of atomic hydrogen before and after the shock passage. These relations reduce to

$$P = \rho_0 a_0^2 \frac{2}{\gamma + 1}M^2 \quad ,$$

$$\rho = \frac{\gamma + 1}{\gamma - 1}\rho_0 \quad , \qquad u = \frac{2}{\gamma + 1}M \quad , \tag{2.19}$$

for the cases $\alpha_0 = \alpha_1 = 0$ ($\gamma = 9/7$) and $\alpha_0 = \alpha_1 = 1$ ($\gamma = 5/3$). These are the ideal-gas shock relations for $M^2 \gg 1$. Plugging these relations into equation (2.13) and ignoring the third term, we get the differential equation

$$\frac{dM}{K(\alpha_0,\alpha_1,M)} = -\frac{d\rho_0(x)}{\rho_0(x)} \quad , \tag{2.20}$$

where

$$K(\alpha_0,\alpha_1,M) = 7/(18F\,[\frac{7}{18}\,GM + a_0FH\,(1 + \frac{GM(16 - F)}{24F^{3/2}})])$$

and

$$G = \frac{18}{7}\,(\frac{7 - \alpha_1}{8}) + \frac{9}{7}\,[2(\frac{7 - \alpha_1}{8})^2\,M^2 + \frac{(\alpha_1 - \alpha_0)(1 + \alpha_1)E}{a_0^2}\,]$$

$$x\left\{[(\frac{7 - \alpha_1}{8})M^2]^2 + \frac{(\alpha_1 - \alpha_0)}{a_0^2}\,(1 + \alpha_1)EM^2\right\}^{-1/2} .$$

To solve this equation the functional dependence of $\alpha_1(M)$ is needed. I used the approximate form $\alpha_1(M) = 0.02\ M^2$ which matches the results of § IV reasonably well. The equation was then numerically integrated for the case $\alpha_0 = 0$ and the results are compared with the solution of Whitham in Figure 3.

VI. Radiation Losses

The preexisting sources of opacity are too weak to cause significant radiation losses within the hot but relatively thin relaxation zone ($\tau \approx 10^{-5}$). Therefore it is necessary for the gas to be in some way excited so that it can radiate effectively. There is a variety of possible ways that this could happen; for example, the rotational-vibrational line spectra of the H_2 molecule and the H_2O molecule will be excited. Furthermore, elements of $z > 2$ can be excited by neutral and

Figure 3. These are solutions of density versus Mach number calculated using the method of G. B. Whitham. Curve 1 is without the effects of dissociation. Curve 2 includes these effects. The dotted line indicates where radiative damping sets in. The sound speed for T = 2000 K $\approx$ 3.4 km s^{-1}.

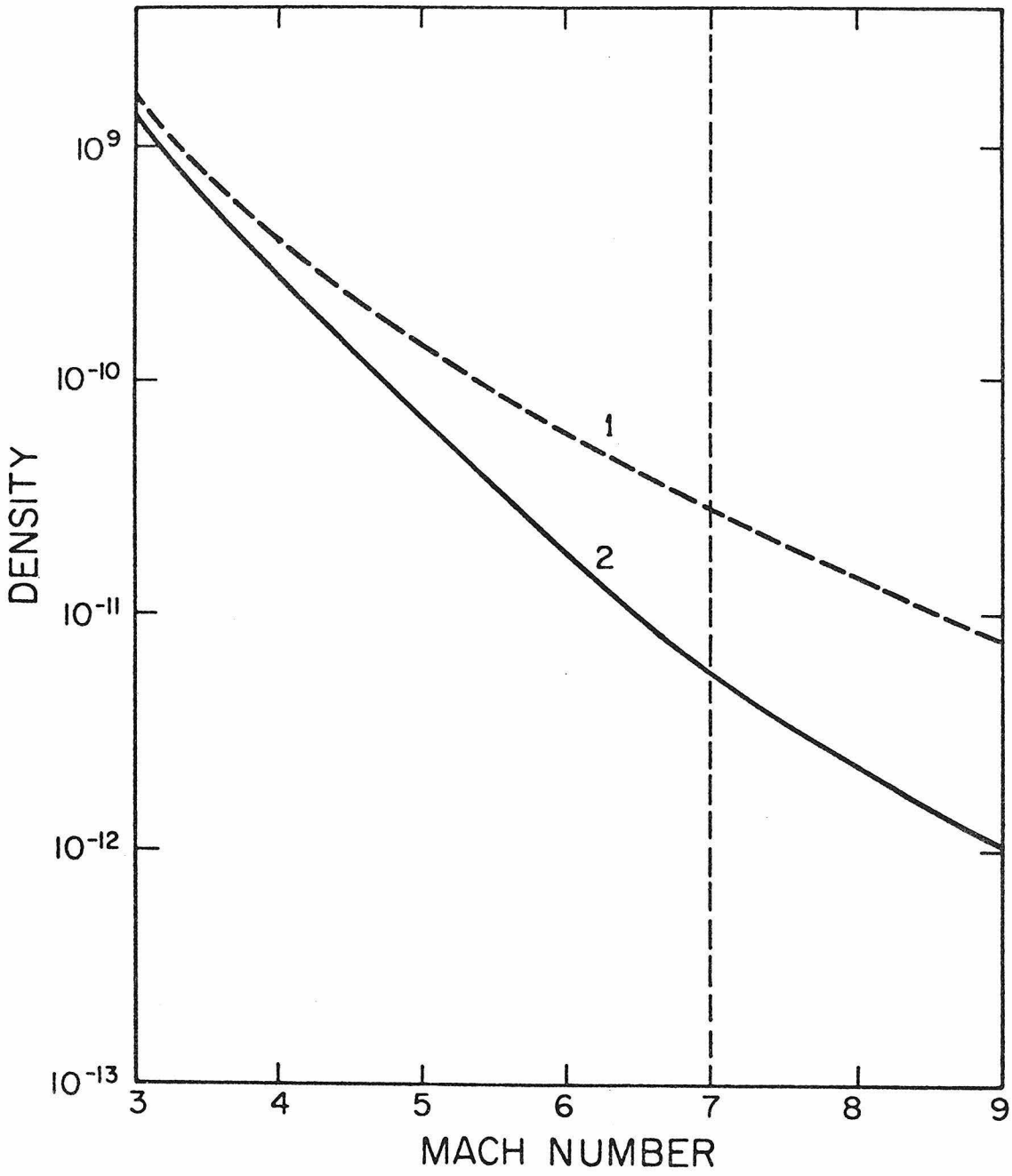

Fig. 3

electron collisions. However, for any mechanism to cause a significant energy loss it must be excited before the dissociation of H_2 molecules has cooled the gas.

The temperature of the gas immediately behind the shock front will be several times 10,000 K. For a shock moving 25 km s^{-1} the temperature will be approximately 50,000 K. As H_2 dissociates the gas temperature will go down to approximately 3000 K. Therefore we want to compare rates for $T > 3000$ K.

Approximate rates for dissociation, ionization, and excitation can be found from the following formula:

$$R = N^2 \langle \sigma v \rangle \left[\frac{u}{kT} + 1\right] e^{-u/kT} \quad (s^{-1}\ cm^{-3}) \tag{2.21}$$

(Zel'dovich and Raizer, 1966), where σ, v, and u are the appropriate cross section, thermal velocity, and excitation or binding energy, respectively.

For the temperature range $250\ K < T < 5000\ K$ the rate for dissociation of H_2 is given approximately by

$$R = 3.6 \times 10^{-10}\ N^2 e^{-48{,}300/T} \quad (s^{-1}\ cm^{-3}) \tag{2.22}$$

(Baulch, 1972), where N is the number density of H_2 molecules. This equation can be extended to higher temperatures by putting in the temperature dependence of the thermal velocity. Doing this, we get

$$R = 7.2 \times 10^{-12}\ T^{1/2}\ N^2 e^{-48{,}300/T} \quad (s^{-1}\ cn^{-3}) \quad . \tag{2.23}$$

For the ionization and excitation rates by electron impact the cross section, σ, is approximately 10^{-17} cm^2 (Zel'dovich and Raizer, 1966); therefore $\langle\sigma v\rangle \approx 6 \times 10^{-12} T^{1/2}$.

Ionization energies for lines in metals are typically greater than 4 eV. Assuming such an excitation energy,

$$R_m \approx 6 \times 10^{-12} T^{1/2} N_e N_m e^{-45,500} \ (s^{-1} \ cm^{-3}) \quad , \tag{2.24}$$

where N_e and N_m are the number density of electrons and metal atoms, respectively. The number density of electrons before passage of the shock wave is approximately 10^{-5} N (Johnson, 1974) and $N_m < 0.003$ N; thus we see that the ionization rate by electron impact is much too slow to affect the electron number density. The excitation rate by electron impact can be found from equation (2.24) by substituting the excitation energy in place of the ionization energy. This energy can be lower than 4 eV. This increases the rate at lower temperatures; however, for T > 3000 K the dissociation rate is still larger.

For ionization and excitation by heavy particles the cross section is much smaller than for electron impact, typically 10^{-20} to 10^{-22} cm^2 (Zel'dovich and Raizer, 1966). Furthermore, the velocities are slower due to their heavier masses. The rate can be expressed as

$$R = (10^{-16} \text{ to } 10^{-18}) T^{1/2} N_m N \quad \exp(-E_x/T) (s^{-1} \ cm^{-3}) \quad . \tag{2.25}$$

This rate is again smaller than the dissociation rate for T > 3000 K.

Rotational and vibrational degrees of freedom of the H_2 molecule are excited; however, the H_2 molecule has no dipole moment and radiates very slowly. The Einstein A coefficients for the 1-0, 2-0, and 3-0 bands are 8×10^{-8}, 2.6×10^{-7}, and 1.1×10^{-7} s^{-1}, respectively. These rates are to be compared with the dissociation rates of approximately 10^{-5} s^{-1} at T = 3000 K and $N = 10^{12}$.

The rotational heat loss rate from the excitation of the H_2O molecule is given by the approximate formula

$$C = NN_{H_2O} \langle \sigma v \rangle h\nu(\exp(-h\nu/kT) - \exp(-h\nu/kT_x))(\text{ergs } s^{-1} \text{ cm}^{-3}) \quad (2.26)$$

(Goldreich and Scoville, 1976), where $h\nu$ is the energy of the rotational photon $\approx$ 0.01 eV, T_x is the excitation temperature and σv is the inelastic rate constant $\approx 2 \times 10^{-11} T^{1/2}$.

For the temperature range T > 3000K, $h\nu/kT \ll 1$. Therefore the expression in brackets can be expanded, and we get

$$C \approx NN_{H_2O} \langle \sigma v \rangle h\nu \left(-\frac{h\nu}{kT} + \frac{h\nu}{kT_x}\right) (\text{ergs } s^{-1} \text{ cm}^{-3}) \quad , \quad (2.27)$$

which is always smaller than

$$C = NN_{H_2O} \langle \sigma v \rangle \frac{(h\nu)^2}{kT} (\text{ergs } s^{-1} \text{ cm}^{-3}) \quad . \quad (2.28)$$

The abundance of H_2O is approximately 10^{-4} N (Goldreich and Scoville, 1976); therefore

$$C_{H_2O} \approx N^2 2 \times 10^{-15} T^{-1/2} \text{ eV s}^{-1} \text{ cm}^{-3} \quad ,$$

which is to be compared with the energy going into dissociation of

$$C_D \approx 3 \times 10^{-11} T^{1/2} N^2 e^{-48,300/T} \text{ eV s}^{-1} \text{ cm}^{-3} \quad .$$

For $T > 3000$ K the rate for dissociation dominates.

From these considerations it is reasonable to ignore radiation losses from within the relaxation zone.

From Figure 2 we see that the postshock zone is left in a cool, unionized state for velocities less than $\sim$25 km s^{-1}. This is because the thermal energy produced after the compression front has gone into dissociating the H_2 molecules. At these low temperatures no strong radiation mechanisms are excited; therefore the shock wave should follow the solution calculated in the last section, which included dissociating effects but neglected radiation effects. Once the shock begins to exceed the velocity of 25 km s^{-1} it has enough energy to totally dissociate the H_2 molecules and leave the final state progressively hotter and more ionized. At this point a multitude of radiation mechanisms become significant. Electrons are no longer rare so that metals are easily excited, bremsstrahlung and recombination radiation occur, and the hydrogen atom itself is excited so that it emits line radiation.

When the radiation losses become comparable to the hydrodynamic power of the stellar pulsations, the shock wave can no longer accelerate. The power supplied is approximately $\dot{E} \lesssim$ PVA, where P = pressure $\approx$

10^2 dyn cm^{-2}, and V = pulsation velocity $\approx 10^6$ cm s^{-1}. Thus $\dot{E}/A$ = 10^8 ergs s^{-1} cm^{-2}. From Figure 3 we see that the density has dropped to approximately 10^{-3} of photospheric density when the shock reaches $V \approx 25$ km s^{-1} and thus the density is approximately 10^{12} cm^{-3}. With a scale height of 10^{11} cm this yields a column density of 10^{23} cm^{-2} and therefore a power supplied to each atom of 10^{-15} ergs s^{-1}. Divide this by the density of electrons ($\sim 10^{12}$ β); we get $10^{-27}/\beta$ ergs cm^{-3} s^{-1}. Cox and Tucker (1969) have calculated the radiation emitted from a plasma of cosmic abundance in the temperature range 10^4 - 10^8 K.

I have expressed the power supplied by the hydrodynamic work in the same units in which Cox and Tucker expressed the energy loss by radiation, so these numbers can be directly compared. At $T \approx 10^4$ K the radiation loss = Power/$\eta_e \eta_H$ is approximately 10^{-24} and rises sharply with temperature. The hydrodynamic power supplied remains larger than this as long as $\beta < 10^{-3}$. From Figure 2 we see that this condition is violated once the shock velocity exceeds a velocity of ~25 km s^{-1}.

The results of Cox and Tucker include line emission, but the column density in Mira variable atmospheres is sufficient for these lines to be optically thick. It is easily seen that bremsstrahlung alone will be sufficient to halt the shock acceleration. From bremsstrahlung the coefficient is 1.64×10^{-27} $T^{1/2}$ β; thus for $\beta > 0.1$ the losses will exceed the power put in. (This occurs at a somewhat higher velocity, ~34 km s^{-1}.)

VII. Mass Loss

An accurate calculation of rate of mass loss by this mechanism would require a fully hydrodynamic atmospheric model calculation. One can very crudely estimate the mass in each ejected shell by assuming that the atmosphere has had time to reestablish equilibrium between shocks. This is a bad approximation, but it should give some insight into the importance of this effect. Assuming an exponential density gradient, the mass in each shell would be approximately $M = 4\pi r_*^2 \rho_0 H$, where ρ_0 is the density where the shocked gas reaches escape velocity and H is the scale height of the atmosphere. From atmospheric models calculated by Johnson (1974) we can estimate these parameters as $\rho_0 \approx 10^{-11}$ to 10^{-12}, $H \approx 10^{11}$, which for a giant yields 10^{-5} to 10^{-6} $M_\odot$ yr^{-1}. From measurements of the masses of dust shells surrounding these stars and the velocity of the gas (Neugebauer, Becklin and Hyland, 1971), a mass loss rate can be estimated to be approximately 10^{-6} $M_\odot$ yr^{-1}. Therefore we see that these numbers are in reasonable agreement.

VIII. Conclusions

Shock waves are observed in the photospheres of Mira variables with velocities less than escape velocity for these stars. These shocks are expected to accelerate as they propagate out from the photosphere up to a velocity not exceeding 25 km s^{-1}, where radiation damping sets in. At this velocity gas behind the shock will have a velocity of approximately 20 km s^{-1}. For stars whose escape velocity is $\leq$20 km s^{-1}

a shell of matter will be puffed from the star each time it expands, leading to a large rate of mass loss.

For stars whose escape velocity is much larger than 20 km s^{-1} or whose surface temperature is larger than 2400 K, this mechanism will not be important.

Finally, this calculation shows that hydrodynamics must be included in model calculations for the atmospheres of these stars.

Acknowledgements

I would like to thank Jim Gunn, Peter Goldreich, and G. B. Whitham for their helpful advice.

REFERENCES

References

Baulch, D., 1972, Evaluated Kinetic Data for High Temperature Reactions, Vol. 1 (London: Butterworth).

Cox, D. P. and Tucker, W. H., 1969, Ap. J., 157, 1157.

Deutsch, A., 1960, Stellar Atmospheres, ed. J. I. Greenstein (Chicago: University of Chicago Press).

Gehrz, R. D. and Woolf, N. J., 1971, Ap. J., 165, 285.

Goldreich, P. and Scoville, N., 1976, Ap. J., 205, 144.

Johnson, H. R., 1974, Model Atmospheres for Cool Stars, NCAR-TN/STR-95, January.

Neugebauer, G., Becklin, E. and Hyland, A. R., 1971, Ann. Rev. Astr. and Ap., 9, 67.

Taylor, G. I., 1946, Proc. Roy. Soc., 186, 273.

Whitham, G. B., 1958, J. Fluid Mech., 4, 337.

Zappala, R. R., Becklin, E. E., Matthews, K. and Neugebauer, G., 1974, Ap. J., 192, 109.

Zel'dovich, Ya. B. and Raizer, Y. P., 1966-1967, Physics of Shock Waves and High-Temperature Phenomena (New York: Academic Press).

Chapter 3

Violent Relaxation and the Infall of Gas into Clusters of Galaxies

Abstract

The infall of gas into clusters of galaxies is considered. Fully time dependent solutions are found numerically which indicate that the temperature distribution of the gas after infall is nearly isothermal. This restores the constraint on the mass of gas outside of clusters ($\Omega_g < .1$) originally proposed by Gott and Gunn (1971).

I. Introduction

Cosmological theories tell us that the fate of the universe depends on the density parameter Ω, the ratio of the average density of the universe over the critical density defined by the formula

$$\rho_c = \frac{3H^2}{8\pi G}$$

where H is the Hubble constant and G is the gravitational constant. If $\Omega \leq 1$ the universe will expand forever and the geometry is open and infinite, but if $\Omega > 1$ the expansion will eventually be reversed by gravity and the geometry is closed and finite.

The density due to galaxies has been estimated to be $\Omega_{gal} \approx 0.06$ which implies that the universe is open (Gott et al., 1974; Gott and Turner, 1976). This estimate should include any unseen matter

within clusters of galaxies because the virial theorem has been used to determine the average mass to luminosity ratio of cluster galaxies. However, material outside of clusters would have gone uncounted. We attempt to put a limit on the quantity of such material if it is in the form of gas. The possibility that this stuff is compact (e.g., stars or black holes) will not be dealt with.

Diffuse X-ray sources have been discovered in a number of clusters of galaxies (e.g., Gursky et al., 1971; Forman et al., 1972; Kellogg et al., 1972). There is strong evidence that the X-rays are produced by thermal bremstrahlung from a hot ($T \approx 10^8$ K) intracluster gas (Lea et al., 1973; Gull and Northover, 1976). Gott and Gunn (1971) suggest that the inferred gas density ($\sim 4 \times 10^{-27}$ gm cm^{-3} for Coma) near the center of clusters puts a severe constraint on the amount of gas outside of the clusters. This constraint depends on the process of cluster formation, which according to the standard scenario is due to the collapse of density perturbations in an approximately homogeneous universe. Gunn and Gott (1972) show that after the collapse of the initial perturbation material will continue to fall onto the cluster. They develop an infall theory and conclude that too much gas would fall into the clusters to be consistent with the X-ray observations if $\Omega_{gas} > 0.1$. Their treatment left out pressure and it is possible that hydrodynamics could impede the infall of gas into the clusters and thus relax this constraint. Various investigators have performed numerical calculations to determine the effects of hydrodynamics (Lea, 1976; Gull and Northover, 1975; Cowie and Perrenod, 1978; Takahara et al., 1976). Lea's results had large oscillations in the central gas density

which are now believed to be due to some numerical instability. The other researchers found that an accretion shock develops near the center of the cluster and travels outward leaving the gas behind the shock hot and relatively quiescent. Cowie and Perrenod (1978) constrain the gas outside of clusters to the value $\Omega_{gas} < 0.2\ (H_o/50\ \text{km s}^{-1}\ \text{Mpc}^{-1})^{-3/2}$. However, Gull and Northover (1975) claim that the temperature distribution of the gas after infall should be adiabatic, i.e., $P\rho^{\gamma}$ = constant throughout. This temperature distribution allows large amounts of gas far from the cluster center and thus reopens the possibility that the density of gas outside of clusters could be sufficiently large to close the universe.

In all of these calculations a fixed gravitational field has been used. However, both the galaxies and the gas were falling inward at the same time. The present calculation includes the time dependence of the gravitational field. This is accomplished by numerically integrating the equations of motion for many self gravitating bodies. Spherical symmetry is assumed which makes the problem one dimensional and thus greatly simplifies the calculations. We find that the qualitative features of the gas infall are not altered; however, the temperature distribution is not that assumed by Gull and Northover. It is instead very nearly isothermal. This is in good agreement with the observations (Lea et al., 1973; Muskotsky et al., 1978) and restores the constraint on the gas outside of clusters to $\Omega_{gas} < 0.1$. Throughout this work we assume a value of 50 km s^{-1} Mpc^{-1} for the Hubble constant,

and the Coma cluster will be used as a prototype because a wide parameter study would be costly, and Coma has been studied in more detail than any other X-ray cluster.

II. The Gravitational Field

All of the gravitational field within the cluster is assumed to be compact masses (galaxies). Furthermore, it is assumed that these masses have formed before the cluster has collapsed. We start the calculation at the epoch of hydrogen recombination ($Z_i \approx 1000$). Before this time the Jeans mass is very large due to the radiation pressure which is coupled to the matter through Thompson scattering (Peebles, 1971). After recombination the Jeans mass drops to about 10^5 $M_\odot$ which is much smaller than the mass of a cluster of galaxies (e.g., $M_{Coma} \approx 10^{15}$ $M_\odot$).

We suppose that there is a spherical region of enhanced density which is slightly larger than the uniform surrounding medium.

The expansion is assumed to be simple Hubble flow

$$V = H_i r \quad ,$$

where H_i is the Hubble constant at this epoch Z_i. The critical density at this time is

$$\rho_{ci} = \frac{3H_i^2}{8\pi G} \quad .$$

Let ρ_{ei} be the external uniform density, which can be expressed in terms of the present deceleration parameter q_o:

$$\rho_{ei} = \rho_{ci} \frac{2(1+Z_i)q_o}{(1-2q_o) + 2q_o(1+Z_i)} ,$$

and

$$H_i^2 \simeq H_o^2 \, 2q_o \, (1 + Z_i)^3 \quad .$$

For a discussion of the generality of this form of initial perturbation see Gunn and Gott (1972).

The average density interior to radius r is larger than ρ_{ci} inside the region of density enhancement and falls toward ρ_{ei} with increased radius. The collapse time in the absence of pressure may be determined from the Friedman solutions and is given by

$$Z_c = \frac{\pi \bar{\rho}_i \rho_{ci}^{\,1/2}}{H_i(\bar{\rho}_i - \rho_{ci})^{3/2}} \approx \frac{\pi \rho_{ci}^{\,3/2}}{H_i(\bar{\rho}_i - \rho_{ci})^{3/2}}$$

(Gunn and Gott, 1972). The collapse time of a shell of matter increases with distance from the central perturbation because the average density decreases. Thus there will always be some material falling into the cluster.

An estimate of the initial density of the central perturbation is made by noting that the collapse time of the perturbation is a constant of order unity times the observed cluster galaxy crossing time. These times are typically a few times 10^9 y (Gott and Turner, 1976).

The radius of the perturbation r_c is determined by the mass of the cluster. We assume that the shape of the perturbation is Gaussian, i.e., $\rho_p = \rho_+ e^{-(r/r_c)^2}$ where ρ_+ is the excess density at the center of the perturbation over the background uniform density.

The treatment of Gott and Gunn breaks down when material which is falling inward passes material which has already travelled through the origin and is now moving outward. The mass interior to such a shell of material is not constant and for that reason the energy of the shell is not conserved. It has been shown that this process leads to a statistical distribution similar to highly non-degenerate Fermi Dirac statistics (Lynden-Bell, 1967). This explains the observed fact that the density distribution of many body systems such as globular clusters, elliptical galaxies, and clusters of galaxies are well approximated by a self gravitating isothermal gas sphere (Rood et al., 1972; King, 1966).

Several investigators have simulated this phenomenon numerically (Hénon, 1964; Peebles, 1970; Bouvier and Janin, 1970). We use the model proposed by Hénon which represents a spherical distribution of point masses by concentric shells which are allowed to pass freely through one another and have no physical rigidity. These shells interact only through their mutual gravitation. The gravitational field on the i^{th} shell is computed from the formula

$$g_i = \frac{G}{r_i^2} \sum_{j<i} (m_j + \tfrac{1}{2} m_i) \quad ,$$

where m_i is the mass of the i^{th} shell. A predictor-corrector method is

used to calculate the velocity and position of the shells. After each time step the velocity of each shell is corrected so that energy is conserved exactly. This method requires that each shell crossing is handled with care. To speed the calculations, two time arrays are assigned to the shells. The first is the time of the next crossing and the second is the present time for that shell. The shells are then advanced in a pairwise fashion computing only the motion of the shells that will cross next. An overall time step is also defined which limits the fractional change in velocity and position of any of the shells. When all of the crossings have been accomplished that occur before this time the rest of the shells are advanced forward in time by this step. This method greatly increases the efficiency of the calculation. Furthermore, previous calculations have conserved energy to only about 0.1% while this method conserves energy to approximately one part in 10^{11} on a CDC 7600. To test the positional accuracy of the shells an initially uniform density was set up with a Hubble velocity flow ($V = Hr$) and compared to the analytic Friedman solutions. The code was accurate to better than one part in 10^5 for a Hubble time.

Galaxies that reach the center of the cluster come out the other side. This is accomplished by using a reflecting sphere near the center. The angular momentum of the shells has been set to zero. In the approximation of spherical geometry, angular momentum may be thought of as a repulsive core. We set the reflecting radius at $r = 10^{23}$ cm which produces an effective core radius of several times this value. This is

Figure 1. The gravitational acceleration due to the shells is plotted against radius for several times in units of 10^{17} secs. The initial perturbation had a mass $M_p = 2 \times 10^{15}\ M_\odot$ and the collapse time $t_c = 1 \times 10^{17}$ sec. The external density parameter $\Omega = 1$.

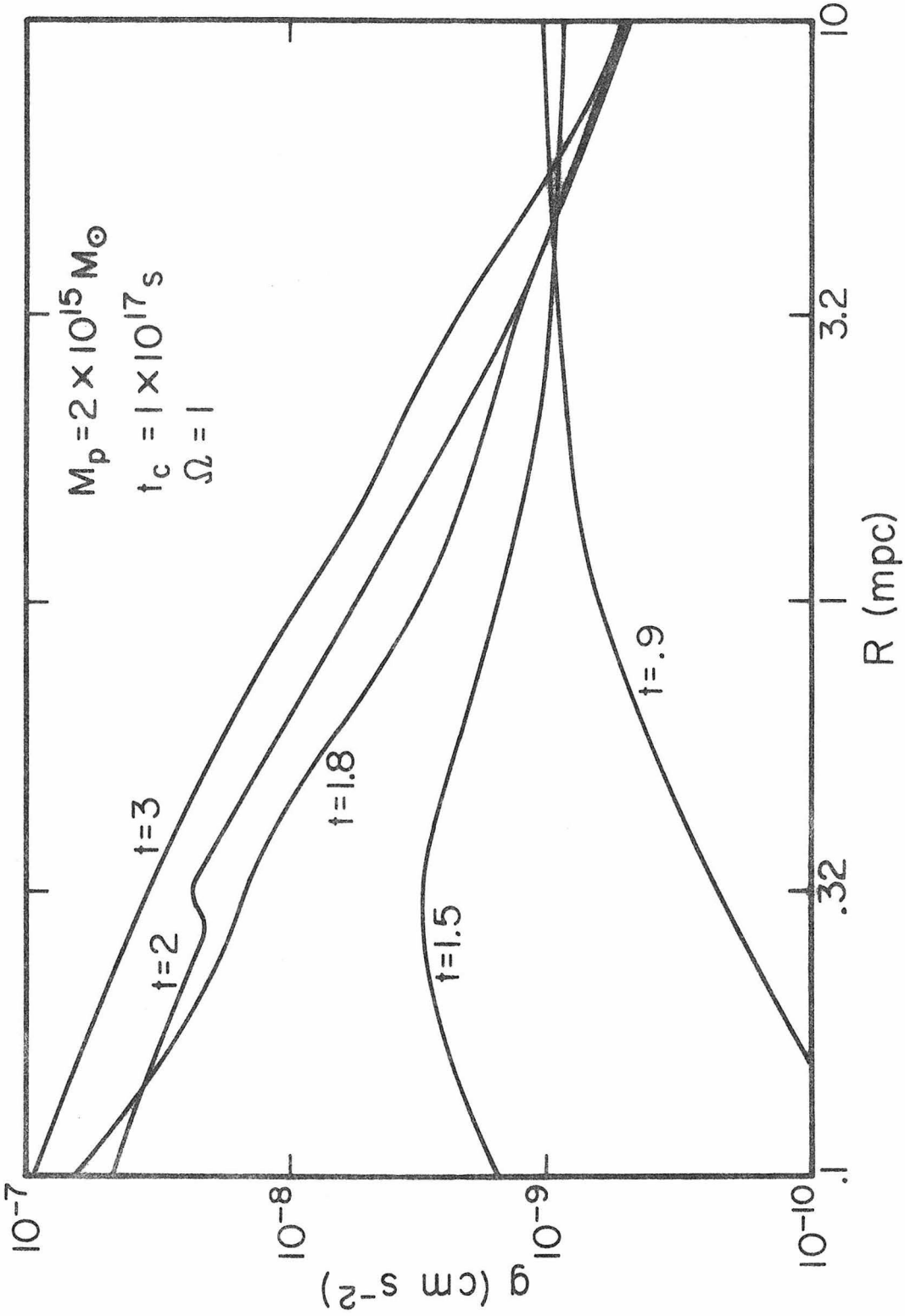
$M_p = 2 \times 10^{15} M_\odot$
$t_c = 1 \times 10^{17}$ s
$\Omega = 1$
t=3
t=2
t=1.8
t=1.5
t=.9
10^{-7}
10^{-8}
10^{-9}
10^{-10}
g (cm s^{-2})
.1
.32
1
3.2
10
R (mpc)

Figure 2. The gravitational acceleration due to the shells is plotted against the radius at the present time for two values of Ω.

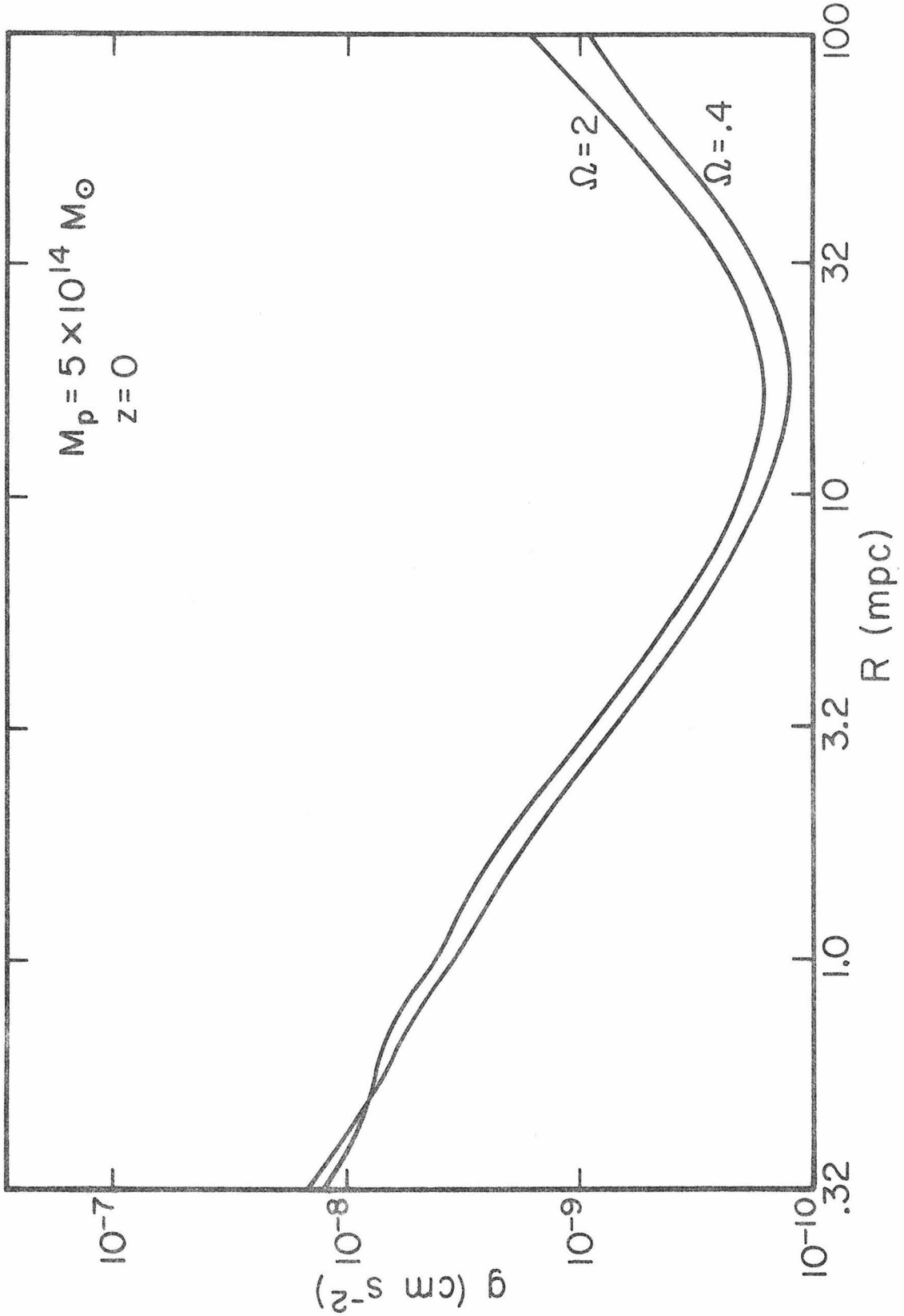
$M_p = 5 \times 10^{14}\ M_\odot$
$z = 0$
$\Omega = 2$
$\Omega = .4$
10^{-7}
10^{-8}
10^{-9}
10^{-10}
g (cm s^{-2})
.32
1.0
3.2
10
32
100
R (mpc)

Figure 3. The velocity of the shells is plotted against their radius at the present time.

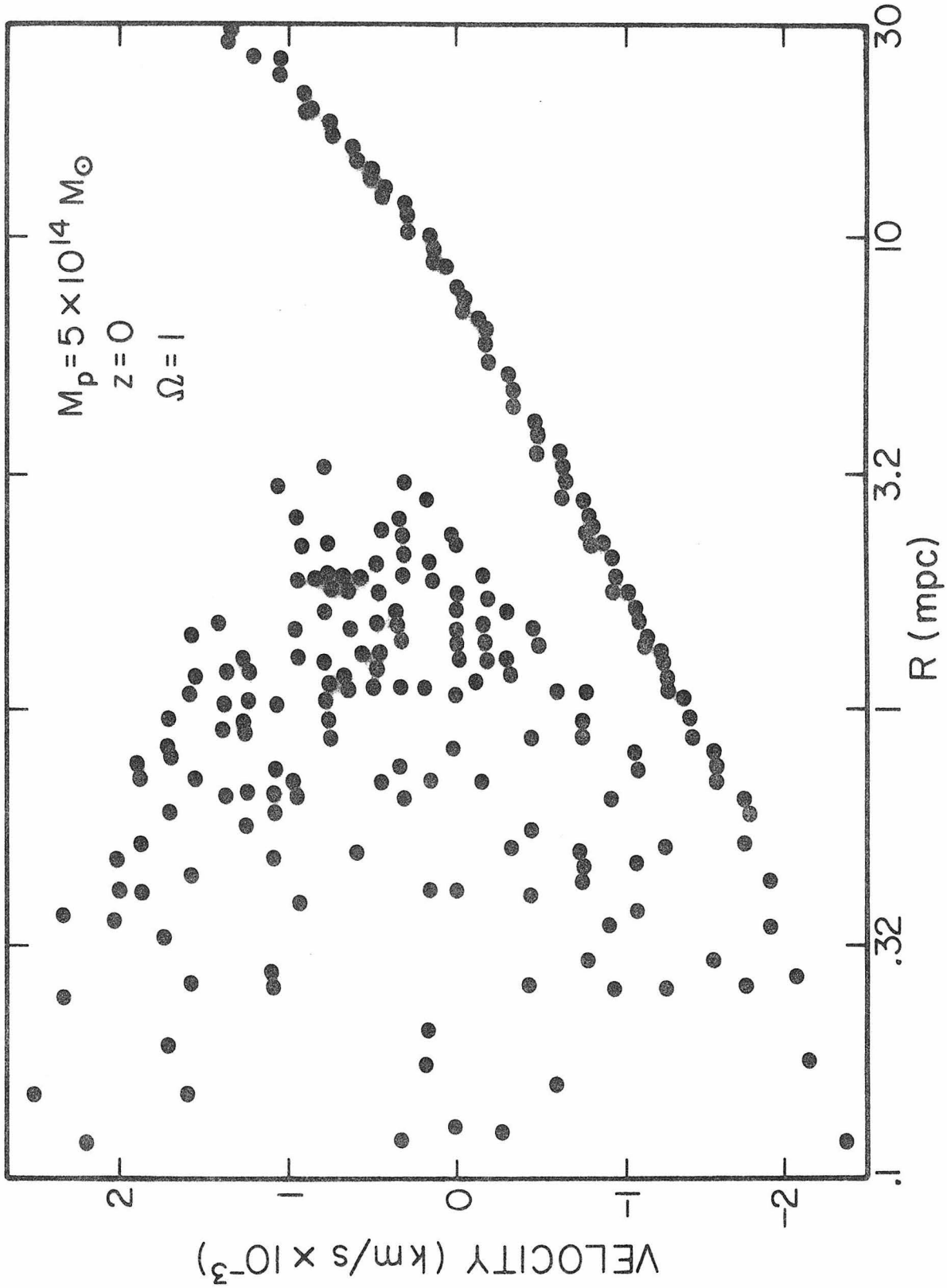
$M_p = 5 \times 10^{14}\ M_\odot$
$z = 0$
$\Omega = 1$
VELOCITY ($km/s \times 10^{-3}$)
2
1
0
-1
-2
.1
.32
1
3.2
10
30
R (mpc)

sufficiently small. This should be compared to the core radius of Coma which is approximately 6×10^{23} cm (Rood et al., 1972).

Three hundred approximately equal mass shells were distributed to mock-up a constant density distribution plus a Gaussian perturbation. The velocities were fixed by the relation $V = H_i r$. The evolution of the collective gravitational field may be seen in Figure 1. The curves approach $g \propto r^{-1}$ as expected. In Figure 2 the final distribution of the gravitational field is compared for different values of the average density background. As expected, a denser universe causes more material to fall onto the initial perturbation and thus the gravitational field is larger. In Figure 3 the velocity of the shells vs. the logarithm of the radius is shown at the present time. As can be seen, the infall is still preceeding at the present epoch.

III. Hydrodynamics

The spherically symmetric Lagrangian hydrodynamic equations are:

Mass conservation:

$$M(r) = \int_0^r 4\pi\, r'^2\, \rho(r')\, dr' \quad ,$$

where $\rho(r)$ is the density at r and $M(r)$ is the mass interior to r.

Momentum conservation:

$$\frac{\partial^2 r(M,t)}{\partial t^2} = -g - 4\pi\, r^2\, \frac{\partial P}{\partial M} \quad ,$$

where g is the acceleration due to gravity and P is the gas pressure.

Energy conservation:

$$\frac{\partial E}{\partial t} + P \frac{\partial V}{\partial t} = 0 \quad ,$$

where E is the specific energy and $V = 1/\rho = 4\pi r^2 \frac{dr}{dM}$ is the specific volume. The equations are put into standard finite difference form employing the technique of artificial viscosity to handle shock waves which was first developed by Von Neuman (see Christy, 1964). The variable r(M,t) is represented by the discrete quantity r_i^n where the index n represents the time t^n and the index i represents the mass M_i interior to r_i^n. The mass between i and i-1 is given by

$$\Delta M_{i-\frac{1}{2}} = M_i - M_{i-1} \quad .$$

The specific volume of the mass element at $i-\frac{1}{2}$ is

$$V^n_{i-\frac{1}{2}} = \frac{4}{3}\pi \{(R_i^n)^3 - (R^n_{i-1})^3\} / M_{i-\frac{1}{2}} \quad .$$

The radius of each gas shell is advanced in time by the equation

$$R_i^{n+1} = R_i^n + \Delta t^{n+\frac{1}{2}} U_i^{n+\frac{1}{2}}$$

where $\Delta t^{n+\frac{1}{2}}$ is the time between t^{n+1} and t^n, and $U_i^{n+\frac{1}{2}}$ is the velocity of the shell i at time $t^{n+\frac{1}{2}}$.

Shock waves are treated by introducing a viscous pressure which is proportional to the compression rate of a mass zone. The Von Neuman artificial viscosity is given by the equation

$$Q_{i-\frac{1}{2}}^{n-\frac{1}{2}} = C_Q \frac{(U_i^{n-\frac{1}{2}} - U_{i-1}^{n-\frac{1}{2}})^2}{(V_{i-\frac{1}{2}}^{n} + V_{i-\frac{1}{2}}^{n-1})} \quad .$$

Large values of C_Q increase the stability of the scheme but spread the shock wave over a large number of zones. Satisfactory stability was achieved with a value of 10. This is somewhat larger than is typically used and helps smooth the noise introduced by the many body code.

The momentum equation is

$$U_i^{n+\frac{1}{2}} = U_i^{n-\frac{1}{2}} - \Delta t^n \left\{ \frac{(g_i^{n+1} + g_i^n)}{2} + \frac{4\pi (R_i^n)^2}{\Delta M_i} \left[P_{i+\frac{1}{2}}^n - P_{i-\frac{1}{2}}^n + Q_{i+\frac{1}{2}}^{n-\frac{1}{2}} - Q_{i-\frac{1}{2}}^{n-\frac{1}{2}} \right] \right\}$$

The boundary conditions are $U_{i=1}^n = 0$ for the inner boundary and it is assumed that at the outer boundary the hydrodynamics is unimportant; thus

$$U_N^{n+\frac{1}{2}} = U_N^{n-\frac{1}{2}} - \Delta t^n \left(\frac{g_N^{n+1} + g_N^n}{2} \right)$$

The gas is assumed to be adiabatic (i.e., no radiation losses or heat conduction). The energy equation is then

$$E^{n+1}_{i+\frac{1}{2}} - E^{n}_{i+\frac{1}{2}} + \left\{ \frac{1}{2} \left[P^{n}_{i+\frac{1}{2}} + P^{n+1}_{i+\frac{1}{2}} + Q^{n+\frac{1}{2}}_{i+\frac{1}{2}} \right] \left[V^{n+1}_{i+\frac{1}{2}} - V^{n}_{i+\frac{1}{2}} \right] \right\} = 0 \quad .$$

The justification for the adiabatic assumption is discussed in section IV. The ideal gas law is used for the equation of state and a mean molecular weight of 1/2 m_p is used because the gas is fully ionized.

The time step is chosen to limit the fractional change in the radius, velocity, pressure, etc. This criterion was varied to check for accuracy and the code was tested against analytic solutions of rarefaction waves, shock propagation, and sound wave propagation with good agreement. The acceleration of the gas due to the gravitational field is computed implicitly and a collapse into a fixed gravitational field was accomplished with a total energy conservation of about 1%. The hydro code was then coupled to the shell code of the last section. Observationally the mass of gas has been estimated to be less than 1/8 of the total mass of the cluster (Lea et al., 1973). Therefore, we assume that all of the gravity is due to the galaxy distribution, which is calculated by the many body code. The gas was given an initially uniform temperature and density distribution. The density is arbitrary and must be scaled to the inferred densities from the X-ray observations. For definiteness it was set to 0.01 ρ_{ci}. The initial gas temperature is also arbitrary as long as the gas temperature just prior to collapse is small compared to the final shock heated temperature ($\sim 10^8$ K). For

numerical ease the initial temperature was set to 10^7 K. The time development for the velocity, temperature, and density are shown in Figures 4-6. As can be seen in Figure 4, a shock wave forms at the center and propagates outward. The jiggling seen to the left of the shock front is caused by fluctuations in the gravitational field that are reduced when the number of shells is increased. Runs with only 100 shells had considerably more noise. The most important features are first, that the gas behind the shock is left relatively quiet (i.e., there are no large oscillations), and secondly, the velocity difference across the shock front remains approximately constant as the shock propagates outward. This results in a nearly isothermal temperature distribution behind the shock, as can be seen in Figure 5. From Figure 6 it is seen that the gas density distribution steepens to approximately $\rho \propto r^{-2}$ which is expected for an isothermal gas sphere. Figure 7 shows the development of the brightness distribution of the X-ray source as a function of time. Since nearly all of the X-rays come from near the center, due to the density squared dependence of bremstrahlung emission, the X-ray source does not change significantly after the shock has travelled a reasonable distance from the center.

Figures 8 and 9 show the variation in the final distribution of the gas density and temperature as a function of the average density of the universe.

The gas density is larger for a larger external gas density Ω, as expected. The difference is not large because the collapse time of the initial perturbation is much smaller than the final collapse of the

Figure 4. The velocity of the gas is plotted against the radius for several times in units of 10^{17} sec.

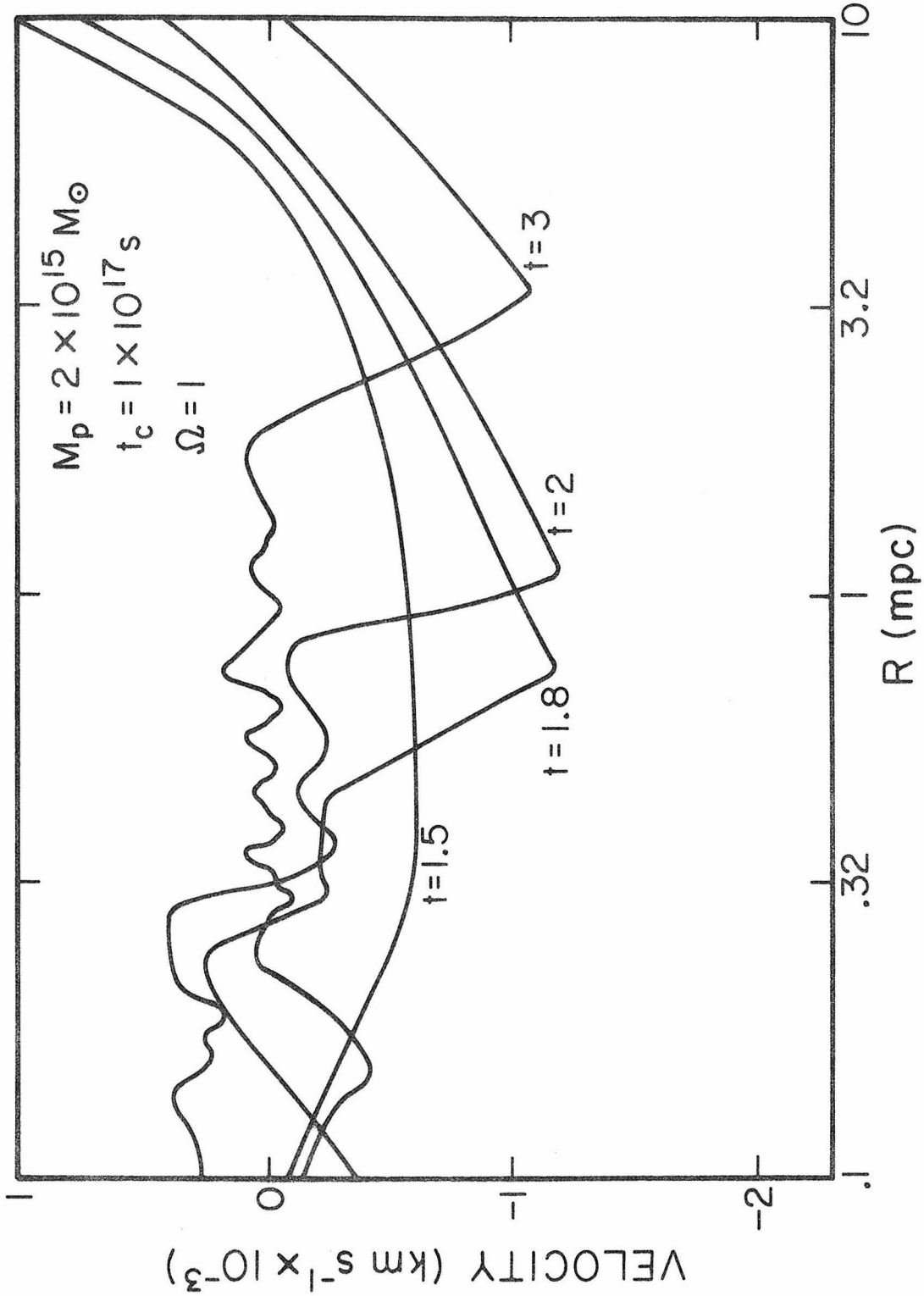
$M_p = 2 \times 10^{15}\ M_\odot$
$t_c = 1 \times 10^{17}$ s
$\Omega = 1$
t=1.5
t=1.8
t=2
t=3
VELOCITY (km s^{-1} x 10^{-3})
R (mpc)
1
0
-1
-2
.1
.32
1
3.2
10

Figure 5. The gas temperature is plotted against the radius at several times in units of 10^{17} sec.

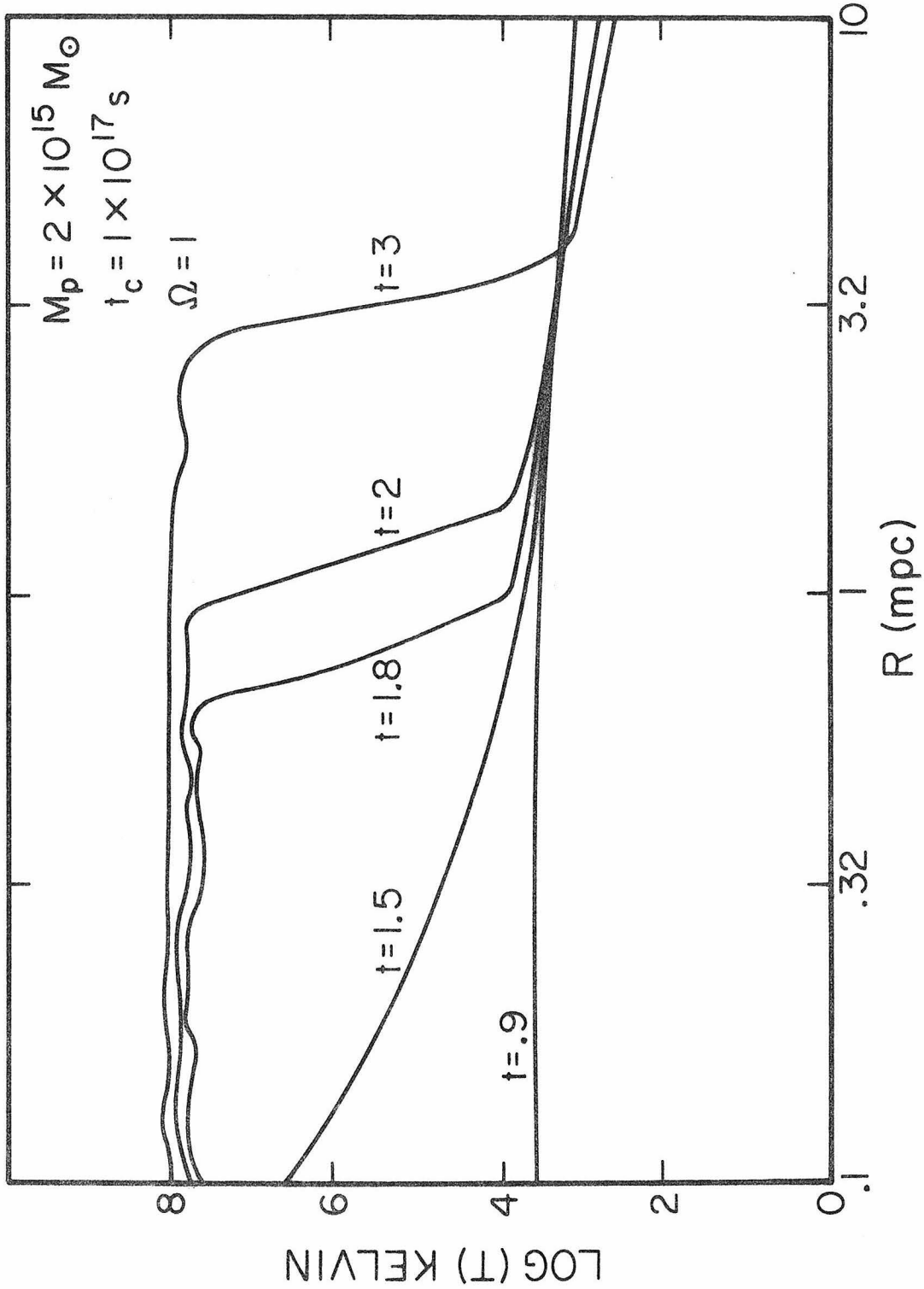
$M_p = 2 \times 10^{15}\ M_\odot$
$t_c = 1 \times 10^{17}$ s
$\Omega = 1$
t=3
t=2
t=1.8
t=1.5
t=.9
LOG (T) KELVIN
8
6
4
2
0
.1
.32
1
3.2
10
R (mpc)

Figure 6. The gas density is plotted against the radius at several times in units of 10^{17} sec.

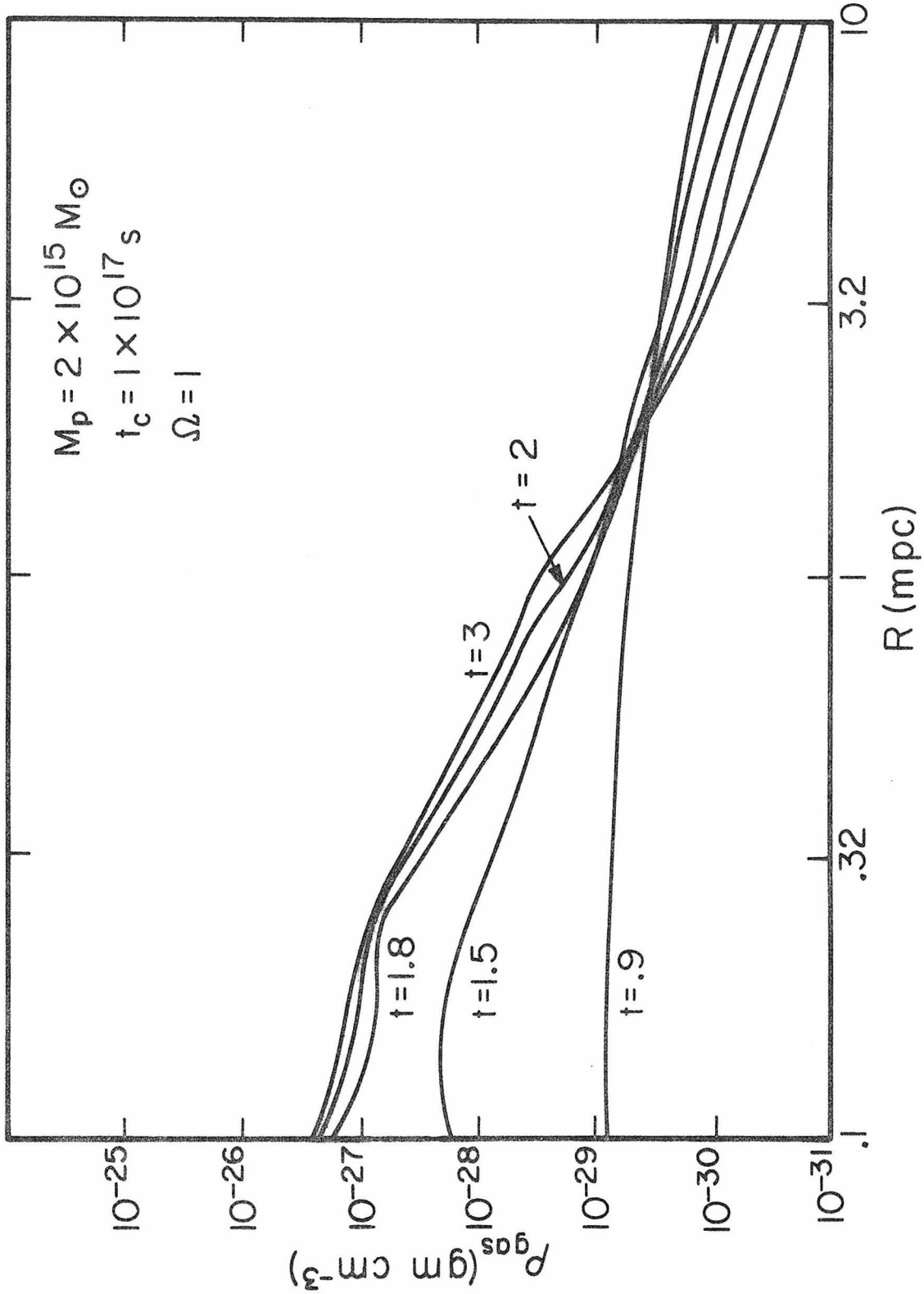
$M_p = 2 \times 10^{15} M_\odot$
$t_c = 1 \times 10^{17}$ s
$\Omega = 1$
t = 2
t=3
t=1.8
t=1.5
t=.9
ρ_{gas} (gm cm^{-3})
10^{-25}
10^{-26}
10^{-27}
10^{-28}
10^{-29}
10^{-30}
10^{-31}
.1
.32
1
3.2
10
R (mpc)

Figure 7. The X-ray brightness of the gas is plotted against the radius at several times in units of 10^{17} sec.

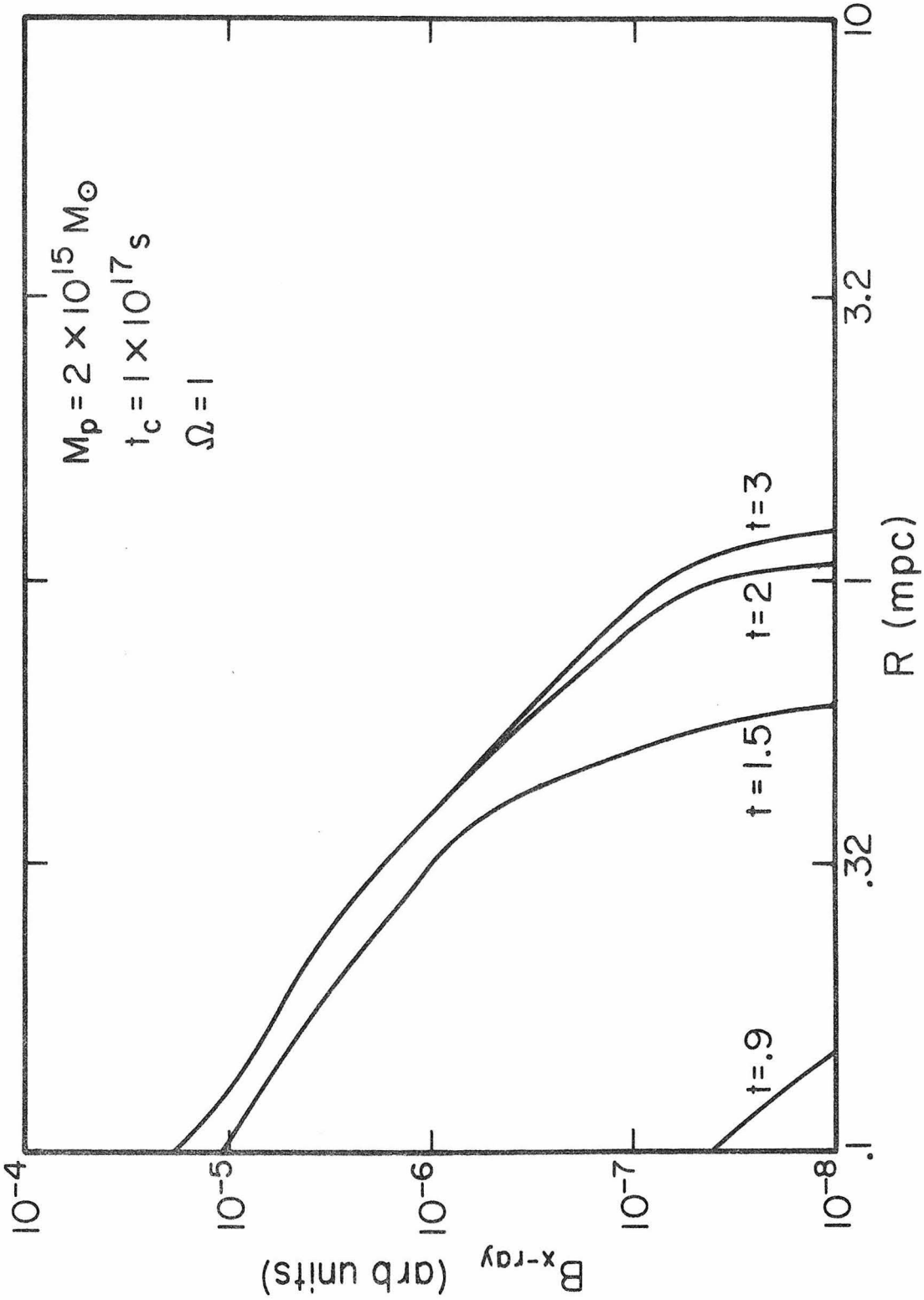
$M_p = 2 \times 10^{15}\ M_\odot$
$t_c = 1 \times 10^{17}$ s
$\Omega = 1$
t=.9
t=1.5
t=2
t=3
10^{-4}
10^{-5}
10^{-6}
10^{-7}
10^{-8}
$B_{x\text{-ray}}$ (arb units)
.1
.32
1
3.2
10
R (mpc)

Figure 8. The gas density is plotted against the radius at the present epoch for two values of Ω.

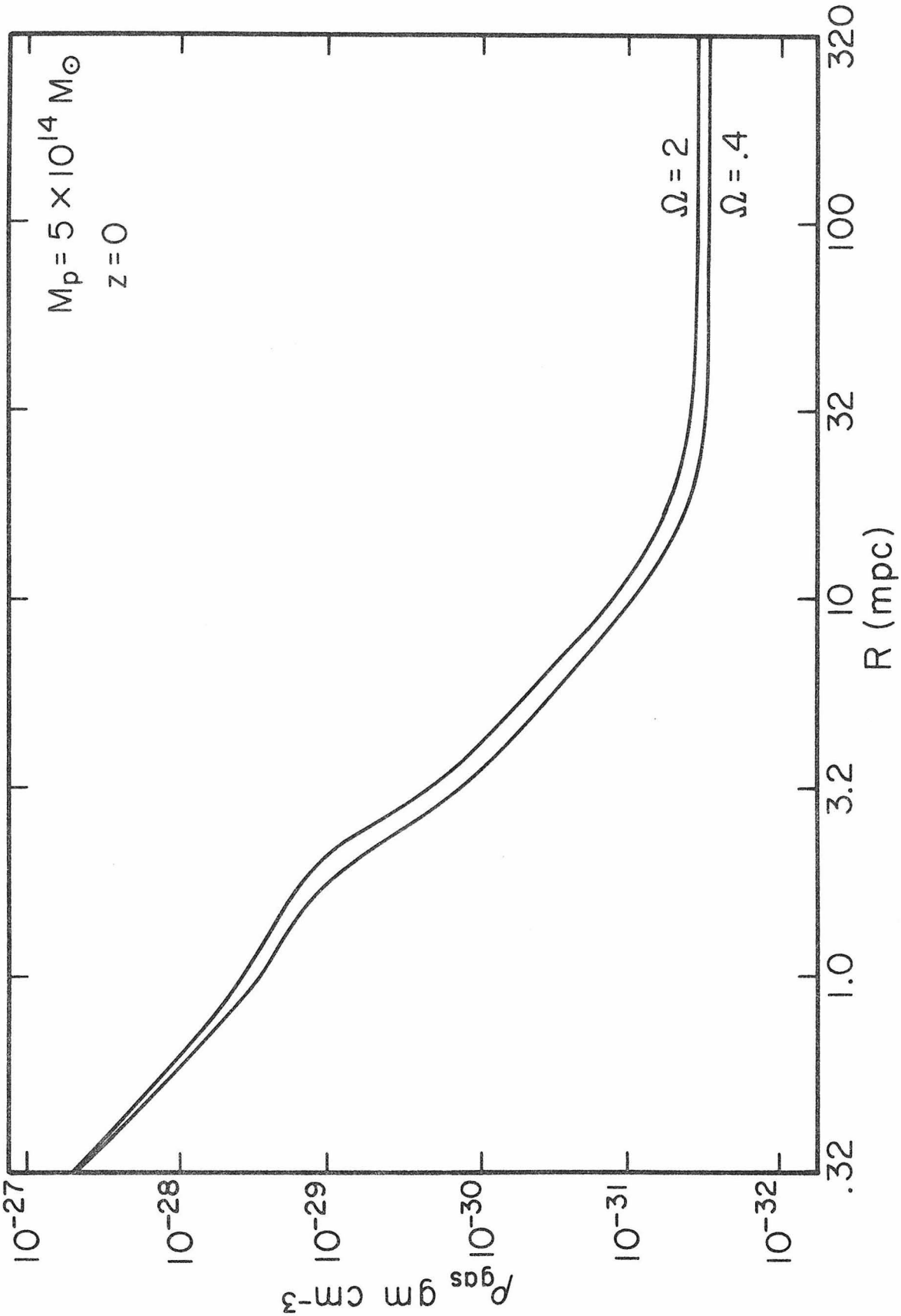
$M_p = 5 \times 10^{14}\ M_\odot$
z = 0
Ω = 2
Ω = .4
ρ_{gas} gm cm^{-3}
10^{-27}
10^{-28}
10^{-29}
10^{-30}
10^{-31}
10^{-32}
.32
1.0
3.2
10
32
100
320
R (mpc)

Figure 9. The gas density is plotted against the radius at the present epoch for two values of Ω.

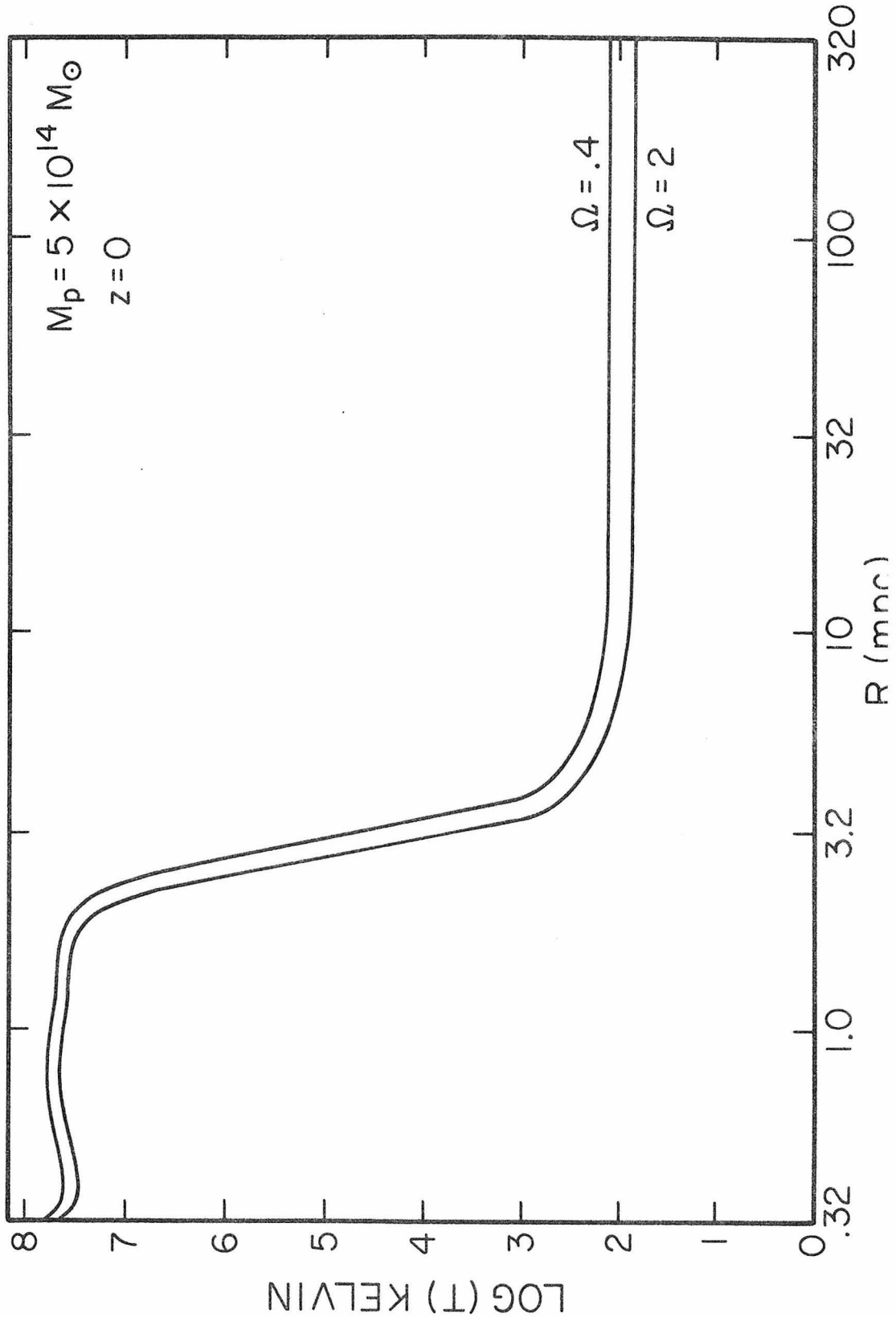
$M_p = 5 \times 10^{14}\ M_\odot$
z = 0
Ω = .4
Ω = 2
LOG (T) KELVIN
R (mpc)
8
7
6
5
4
3
2
1
0
.32
1.0
3.2
10
32
100
320

universe if $\Omega \leq 2$. The temperature is lower for larger values of Ω. This is because more material falls into the cluster after the initial perturbation collapses and this material is more loosely bound.

IV. Discussion

Gull and Northover (1975) argue that the infall of gas leads naturally to an adiabatic distribution, i.e., a polytrope of index $\gamma = 5/3$ ($P_\rho^\gamma = \text{const}$). With this assumption they find static solutions in the cluster potential well. The gas temperature decreases with radius and therefore the gas density does not decrease with radius as fast as it does in the isothermal case. This leads to their conclusion that there could enough gas outside clusters to close the universe. In contrast, the present calculations indicate that the temperature distribution is nearly isothermal after infall. The difference comes from their assumption of a static gravitational field as compared to the present fully time dependent calculation. For the static case gas which falls into the center of the cluster obtains the highest free fall velocity and consequently is shock heated to the highest temperature.

The potential energy change for the infalling material is a monotonically decreasing function of the radius at which it encounters the accretion shock. Therefore the final temperature decreases with radius. However, in the time dependent case the depth of the well is increasing as the accretion shock moves outward. Figures 10 and 11 show the cluster mass and the accretion shock radius as a function of time. The increase in the depth of the well causes the infall velocity

Figure 10. The mass of the cluster is plotted versus time.

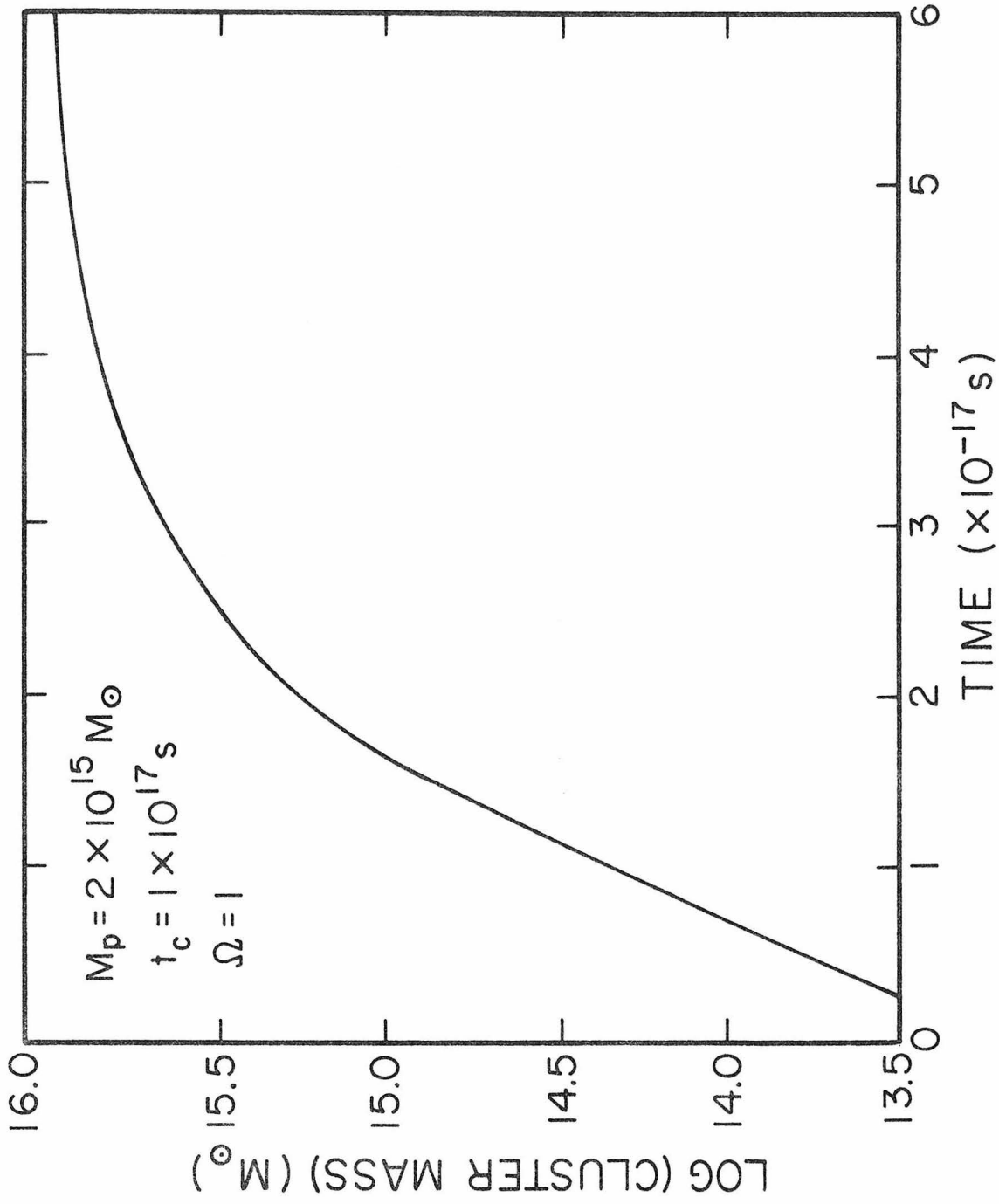
LOG (CLUSTER MASS) ($M_\odot$)
16.0
15.5
15.0
14.5
14.0
13.5
0
1
2
3
4
5
6
TIME ($\times 10^{-17}$ s)
$M_p = 2 \times 10^{15} M_\odot$
$t_c = 1 \times 10^{17}$ s
$\Omega = 1$

Figure 11. The radius of the accretion shock is plotted versus time.

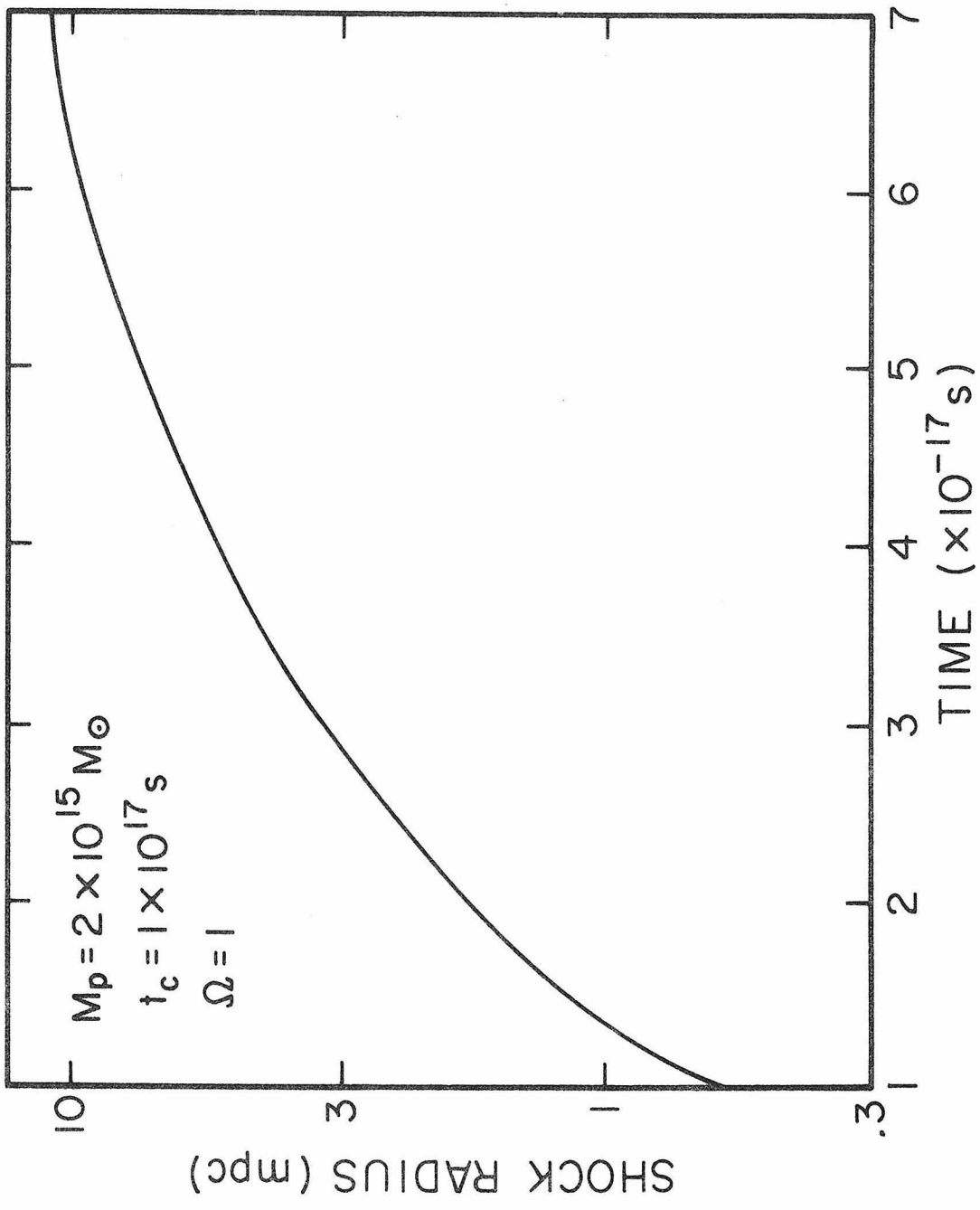
SHOCK RADIUS (mpc)
10
3
1
.3
TIME (×10⁻¹⁷s)
1
2
3
4
5
6
7
Mp = 2×10¹⁵ M⊙
tc = 1×10¹⁷ s
Ω = 1

to be nearly constant at the accretion shock (see Fig. 4) and thus the final temperature is nearly constant. In fact, the temperature decreases by less than a factor of two out to a radius of 3 Mpc (see Fig. 5). The constancy of the final temperature is probably not just an accident, but must be a result of the near self similarity of the problem. Lea et al. (1973) find that isothermal gas ($\sim 10^8$ K) with a density distribution of the form $\rho = \rho_o (a_o^2 + r^2)^{-3/2}$ or $\rho = \rho_1 (a_1^2 + r^2)^{-1}$ fit the X-ray observations very well. The density distribution that we obtained is well described by the second distribution (see Fig. 8). They find $\rho_1 \approx 4 \times 10^{-3}$ cm^{-3} and $a_1 = 7'$ which is 0.25 Mpc for a distance of 140 Mpc to the Coma cluster. Scaling the density distribution of Figure 8 to these parameters yields $\rho_\infty \approx 5 \times 10^{-31}$ which implies that the total density of the universe from gas outside of the cluster is about $\Omega_{gas} \lesssim 0.1$. More recently observations have been made of X-ray sources in a number of compact clusters (Mushotsky et al., 1978). These authors claim that an adiabatic index $\gamma = 1.1$ fits the data the best, which is in good agreement with our results.

Radiative cooling is dominated by thermal bremstrahlung. The cooling time is approximately

$$\tau_{cool} \approx \frac{7 \times 10^7}{n} \; T_8^{\frac{1}{2}} \; y$$

where T_8 is the temperature in units of 10^8 K and n is the density of hydrogen atoms per cubic centimeter. The central gas density is a

monotomically increasing function of time as can be seen in Figure 6. The present density at the center of Coma is approximately 4×10^{-3} cm^{-3} (Lea et al., 1973). Therefore, cooling has never been important. This justifies the omission of cooling from the calculation.

Furthermore, the effect of electron thermal conduction has been neglected. This is almost certainly justified since the final distribution is nearly isothermal; and furthermore, a magnetic field larger than $\sim 10^{-18}$ gauss will quench electron thermal conduction unless the coherence length of the field is comparable to the size of the cluster. Unfortunately the strength and structure of the intergalactic magnetic field is unknown.

There has been some debate over the origin of the gas within clusters of galaxies because of the discovery of an iron line in the X-ray spectrum (Mitchell et al., 1976). The implied metallicity is approximately solar, which has caused several authors to speculate that nearly all of the gas has been processed and must come from the galaxies (see, e.g., Cowie and Perrenod, 1978).

The possibility of sinks and/or sources of gas can affect our results in three ways. First, if the galaxies absorb more gas than they spit out we may have underestimated the possible gas density outside of the clusters. This possibility was checked by running a model where just as the cluster was beginning to collapse the gas within the original density perturbation was reduced by a factor of ten. The final gas distribution was only slightly altered with ρ_0/ρ_∞ reduced by about a

factor of 2. This would increase the density estimate outside of clusters to approximately $\Omega_{gas} < 0.2$.

Second, if the galaxies produce more gas than they absorb the estimate for the gas outside would be too large.

Third, the gas ejected by galaxies might be cooler than the gas within the cluster. This would cause a slow flow of gas inward until adiabatic compression heated the gas sufficiently for it to come to hydrostatic equilibrium. This possibility is unlikely because the galaxies are moving through the intracluster medium and the gas ejecta should shock heat to the appropriate temperature.

Note that it is not necessarily true that the observation of iron within the cluster sources indicates that all of this material is of cosmic abundance. This is because the observations are mainly sensitive to the center of the cluster, since the gas density is proportional to r^{-2} and thus the projected emission is proportional to r^{-3}. Furthermore, if ram pressure stripping is the most important ejection mechanism we expect this material to be preferentially deposited near the center because the gas density is so much higher there.

Gisler (1976) has numerically calculated the effectiveness of ram pressure stripping under various conditions. His results indicate that a galaxy near the core of the Coma cluster should retain less than 1% of the gas which is ejected by its stars. At a distance of approximately 1 Mpc from the center approximately 10% is retained and at 2 Mpc from the center a galaxy shoud be able to maintain nearly all of its gas. Note that in the past, when the density of gas within the cluster

was lower, the effect of ram pressure stripping was even more centralized. Since the effective radius of the Coma cluster is ~6Mpc previous estimates of the total mass of iron in clusters must be reduced by at least a factor of 3. The observations imply that (Fe/H) $\sim 1.4 \times 10^{-5}$ which is approximately one half of the solar value (Mushotsky et al., 1978). This implies a total mass $M_I \lesssim 2 \times 10^9 M_\odot$ of iron. Thus there is no problem here as there has been with the previous larger estimates of the total mass of iron.

Finally, we predict that the ratio of the iron line intensity over the X-ray intensity should decrease with distance from the center of clusters. This ratio should approach zero at about 2 Mpc from the center. The detection of such a gradient would support the view that most of the gas within clusters is primordial in nature.

V. Conclusions

We conclude that the temperature of gas after infall into clusters of galaxies is nearly spatially constant. This is due to the deepening of the gravitational potential well as the accretion shock moves outward. This reestablishes the constraint on the quantity of gas outside of clusters of galaxies ($\Omega_{gas} \lesssim 0.1$) first suggested by Gott and Gunn (1971) which they derived from the gas density within clusters of galaxies inferred from X-ray observations.

It is suggested that a test for the primordial origin of the gas within clusters of galaxies can be made by looking for a gradient

in the ratio of the iron line over the X-ray flux as a function of distance from the cluster center.

Acknowledgements

I would sincerely like to thank Dr. James E. Gunn for suggesting this problem to me, for encouraging me throughout its completion, and expanding my picture of what the universe is like.

References

Bouvier, P., and Janin, G. 1970, Astr. and Ap., 5, 127.

Christy, R. F. 1964, Reviews of Modern Physics, Vol 36, 555.

Cowie, L. L., and Perrenod, S. C. 1978, Ap. J. 219, 354.

Forman, W., Kellogg, E., Gursky, H., Tananbaum, H., and Giacconi, R. 1972, Ap. J. 178, 309.

Gisler, G. R., 1976, Astron. and Astrophys. 51, 137.

Gott, J. R. and Gunn, J. E. 1971, Ap. J. (Letters) 169, L13.

Gott, J. R., Gunn, J. E., Schramn, D. N., and Tinsley, B. M. 1974, Ap. J. 194, 543.

Gott, J. R. and Turner, E. L. 1976, Ap. J. 209, 1.

Gunn, J. E. and Gott, J. R. 1972, Ap. J. 176, 1.

Gull, S. F. and Northover, K. J. E. 1975, M.N.R.A.S. 173, 585.

Gursky, H., Kellogg, E., Murray, S., Leong, C., Tananbaum, H., and Giacconi, R. 1971, Ap. J. (Letters) 167, L81.

Hénon, M. 1964, Ann. d'Ap. 27, 83.

Kellogg, E., Gursky, H., Tananbaum, H., Giacconi, R., and Pounds, K. 1972, Ap. J. (Letters) 174, L65.

King, I. R. 1966, A. J. 71, 64.

Lea, S. M. 1975, Ap. Letters, 16, 141.

_____ 1976, Ap. J. 203, 569.

Lea, S. M., Silk, J., Kellogg, E., and Murray, S. 1973, Ap. J. (Letters) 184, L105.

Lynden-Bell, D. 1967, M.N.R.A.S. 136, 101.

Mitchell, R. J., Culhane, J. L., Davison, P. J. N., and Ives, J. C. 1976, M.N.R.A.S. 176, 29P.

Mushotsky, R. F., Serlemitsos, P. J., Smith, B. W., Boldt, E. A., and Holt, S. S. 1978, Ap. J. 225, 21.

Peebles, P. J. E. 1970, A. J. 75, 13.

_____ 1971, "Physical Cosmology." Princeton University Press, eds. Arthur S. Wightman and John J. Hopfield.

Rood, H. J., Page, T. L., Kintner, E. C., and King, I. R. 1972, Ap. J. 175, 627.

Takahara, F., Ikeuchi, S., Shibazaki, N., and Hoski, R. 1976, Progr. Theor. Phys. 56, 1093.